Efficient Computation of European Option Prices and their Sensitivities with the Complex Fourier Series Method

Abstract

Highly accurate approximation pricing formulae and option Greeks are obtained for European-type options using a complex Fourier series. We assume that risky assets are driven by exponential Lévy processes and affine stochastic volatility models. We provide a succinct error analysis to demonstrate that we can achieve an exponential convergence rate in the pricing method in many cases as long as we choose the correct truncated computational interval. As a novel pricing method, we also numerically demonstrate that the complex Fourier series performs either favourably or comparably with existing techniques in numerical experiments.

JEL classification: G12; G13

Keywords: Complex Fourier series; European options; exotic options; forward contracts; futures; Lévy processes; affine stochastic volatility

1. Introduction

A number of empirical studies suggest that a risky asset's log return exhibits asymmetric leptokurtosis (Rubinstein, 1985, 1994; Bates, 1991, 1996). In other words, the log return is skewed to the left and has a higher peak and two heavier tails than a normal distribution. Moreover, Rubinstein (1985, 1994) indicate that the implied volatility tends to rise for options that are deeply in(out)-of-the-money. This attribute is famously called the volatility smile. Due to these two distinctive empirical attributes, the Black-Scholes model, which assumes that a risky asset's log returns follow a normal distribution and have constant volatility, is not realistic enough to model option prices in financial markets. To improve on the Black-Scholes model in asset pricing, a vast array of models, such as time-changed Brownian motions (e.g., Variance Gamma process Madan and Seneta 1990; Madan and Milne 1991; Madan et al. 1998), have been proposed to incorporate asymmetric leptokurtic asset log returns. Moreover, to model the volatility smile in option pricing, popular models, e.g., affine stochastic volatility and affine jump-diffusion models (Duffie et al., 2000) and models based on Lévy processes, have been developed and adopted in financial practice. Most of these new models (apart from the Merton jump-diffusion (Merton, 1976) and variance gamma Madan and Seneta 1990; Madan and Milne 1991; Madan et al. 1998) do not have a closed-form probability density function (PDF) but a corresponding analytical characteristic function. Thus, option pricing is now more challenging than ever. To price options using the new models, different

numerical methods are naturally employed. According to their popularity, we can roughly classify these methods into three categories: Monte Carlo simulation, finite difference (FD) schemes and Fourier transform methods.

Among the three categories, Monte Carlo methods are the easiest to implement. However, the disadvantage of using Monte Carlo methods is that their approximations always contain some randomness, whereas a closed-form formula will always yield the same result (cf. Carmona and Durrleman, 2003). Furthermore, the fast numerical simulation of Lévy trajectories is itself a non-trivial problem. Monte Carlo simulation may not be exactly correct, as it suffers from simulation error and potential errors in the least-squares method for American options under a Lévy process as reported by Longstaff and Schwartz (2001).

The FD method is another fairly popular numerical method of option pricing when, prior to the exercise, the prices satisfy a certain partial differential equation (PDE), such as the classical Black and Scholes equation, or a partial integro-differential equation (PIDE), such as the classical Black and Scholes equation with an infinite integral term (cf. Andersen and Andreasen, 2000; Almendral, 2004; d'Halluin et al., 2004; Hirsa and Madan, 2004; Almendral and Oosterlee, 2005, 2006, 2007; Cont and Voltchkova, 2005; d'Halluin et al., 2005; Ikonen and Toivanen, 2007a,b; Wang et al., 2007; Tankov and Voltchkova, 2009; O'Sullivan and O'Sullivan, 2013). The general disadvantage of these methods is that they can guarantee only algebraic convergence rates (e.g., Hirsa and Madan, 2004; d'Halluin et al., 2005; Almendral and Oosterlee, 2007), in contrast to Fourier transform methods (Fang and Oosterlee, 2008), which ensure exponential convergence rates in many stochastic processes. Furthermore, using an FD scheme to discretise the integral in the pricing PIDE may not be an ideal algorithm. The FD scheme works well if the Lévy measure is integrable, corresponding to a process of finite intensity, but fails to perform if the integral has a non-integrable singularity at 0. In that case, the integral is generally divided into a local part containing the singularity of the Lévy measure and a non-local part that can be handled by classical quadrature techniques, such as the trapezoidal rule. The discretisation of the local part is more delicate and in the most general case requires a second-order Taylor expansion of the unknown function. The contribution of the small (or smallest) jumps is sometimes approximated by effective diffusion terms (Cont and Voltchkova, 2005; Wang et al., 2007), although this procedure is criticised by Levendorskiĭ (2004) and Kudryavtsev and Levendorskiĭ (2009), who argue that it can lead to sizeable numerical errors. Also working in the FD context, Almendral and Oosterlee (2007) rewrite the PIDE as a sum of two weakly singular Volterra operators through an integration by parts and use established (but quite involved) numerical techniques to address the latter. Their method shows second-order convergence in numerical experiments with finite variation Lévy processes from the CGMY class (Carr et al., 2002), but at present, this approach does not apply to infinite variation processes. As the FD scheme is not a good numerical method to solve PIDE under infinite variation processes, a series of papers using a radial basis function (RBF) interpolation scheme were proposed by Chan and his colleagues to solve a PIDE pricing formula (Brummelhuis and Chan, 2014; Chan and Hubbert, 2014;

Chan, 2016). Specifically, Brummelhuis and Chan (2014) use a multi-quadric as a basis function to compute the action of the integral operator on a single function. Since the radial basis function is explicit, they can exploit its properties to explicitly de-singularise the integral and convert it to a form that is amenable to classical quadrature techniques. In that paper, a second-order convergence rate is achieved in numerically pricing both American and European options.

Fourier transform methods for European options were introduced by Carr and Madan (1991). Their main focus was on pricing a single asset option under the VG model with the fast Fourier transform (FFT). Their basic framework has since been adapted to a variety of option payoffs and a host of asset return models for which the characteristic function is known. In their work, they also provide a solution for solving singularities occurring in the Fourier transform of an non-integrable payoff function. This monumental contribution inspired the later research of Lewis (2001), Lipton (2002) and Lord et al. (2008). Among the Fourier transform methods, those of Oosterlee and his collaborators have attracted considerable attention (Fang and Oosterlee, 2008, 2009, 2011; Leentvaar and Oosterlee, 2008; Ruijter et al., 2013; Zhang and Oosterlee, 2013; Ruijter and Oosterlee, 2015). In their work, they adopt the Fourier cosine series (COS) to price options or derivatives that have different contingency claims and are characterised by path dependence and/or early exercise features. The implementation of the methods is relatively simple but elegant and is capable of pricing options under different stochastic processes as long as their characteristic function exists. The main achievement of these methods is that they can, in many cases, maintain an exponential convergence rate when pricing options, e.g., European options. Moreover, the methods also exhibit the ability to accurately price options under infinite variation processes.

As an alternative to the COS method and other Fourier transform methods, the complex Fourier series (CFS) we propose in this paper is intended to derive highly accurate approximation pricing formulae for European-type options under exponential Lévy processes and affine stochastic volatility models. The main contribution of the method is that it not only retains an exponential convergence rate in European option prices with fewer Fourier terms but also is as accurate as or even better than the COS method. Like the COS method, the CFS method can price options accurately under infinite variation processes, whereas the FD method fails to do so. Unlike the Monte Carlo methods, the CFS method can avoid randomness in its pricing solution because of closed-form pricing formulae. Finally, we do not limit ourselves to a pricing formula for a European vanilla option but formulate a more generalised formula for any option that has a complex payoff structure, such as asymmetric/symmetric power option payoffs or an option on a forward or futures contract. Based on the approximation pricing formulae, we also derive the Greeks, the quantities representing the sensitivity of the price of options.

This paper is organised as follows. Section 2 reviews the basic properties of the characteristic function of a stochastic process and complex Fourier series. Section 3 investigates how to construct a truncated interval to gain greater accuracy in the CFS method with less computational resources, establishes the CFS approach and applies it to European-type options. In section 4, we derive the

CFS expression of payoff functions and the Greeks. We conduct an error analysis in section 5. Section 6 presents numerical examples using European-type options. In particular, we contrast the proposed scheme with the COS method and the CONV method. We conclude in section 7 and present the financial stochastic models and some of their cumulants in Appendix A and Appendix B, respectively.

2. A Crash Course in Characteristic Functions and Complex Fourier Series

In this section, we briefly introduce some important properties of the characteristic functions of random variables and classical complex Fourier series. For further details, we refer readers to Boyd (2003), Schoutens (2003) and Cont and Tankov (2004).

2.1. Characteristic Functions and Their Properties

The characteristic function $\phi_X(z) = \mathbb{E}\left[e^{izX}\right]$ of a real-valued random variable X is defined for arbitrary real numbers z as the expectation of the complex valued transformation e^{izx}, where $i = \sqrt{-1}$ is the imaginary unit. If $f_X(x)$ is the PDF of the random variable, then the integral is

$$\mathbb{E}\left[e^{izX}\right] := \phi_X(z) = \int_{-\infty}^{+\infty} e^{ixz} f_X(x) dx, \quad z \in \mathbb{R}. \tag{1}$$

At a given z, $\phi_X(z)$ is a single random variable. Some properties of characteristic functions are that $\phi_X(0) = 1$ and $|\phi_X(z)| \leq 1$. Moreover, the characteristic function always exists and is continuous. Most important, $\phi_X(z)$ uniquely determines $f_X(x)$. Because the PDF decays to zero as $x \to \infty$, we can truncate the infinite integration to $[a, b] \in \mathbb{R}$ without losing significant accuracy, i.e.,

$$\mathbb{E}[e^{izX}] := \phi_X(z) \approx \int_a^b e^{izx} f_X(x) \mathrm{dx}. \tag{2}$$

We discuss the choice of $[a, b]$ in section 4. If X has kth moment ($k \in \{0, 1, 2, \ldots\}$) satisfying the condition $\mathbb{E}[|X|^k] \leq \infty$, then the moment-generating function is

$$\mathbb{E}[X^k] = \frac{1}{i^k} \frac{\mathrm{d}^k \phi_X(z)}{\mathrm{d}z^k}\bigg|_{z=0}. \tag{3}$$

Furthermore, if we set z equal to iu, where $u \in \mathbb{R}$, we have a different form of (3) such that

$$\mathbb{E}[X^k] = \frac{\mathrm{d}^k \phi_X(-iu)}{\mathrm{d}u^k}\bigg|_{u=0}. \tag{4}$$

In a similar fashion, the cumulants c_k of X can be defined via the following cumulant-generating function:

$$c_k = \frac{1}{i^k} \frac{\partial^k \log \phi_X(z)}{\partial z^k}\bigg|_{z=0}. \tag{5}$$

Finally, as characteristic functions turn convolution into multiplication (cf. Lukacs, 1987), if X and Y are two independent random variables with characteristic functions $\phi_X(z)$ and $\phi_Y(z)$, respectively, then the characteristic function of $X + Y$ is given by $\phi_{X+Y}(z) = \phi_X(z)\phi_Y(z)$.

2.2. Complex Fourier Series

A periodic function $f(t)$ defined on an interval $[-\pi, \pi]$ that has a CFS representation must satisfy the Dirichlet conditions:

1. $f(t)$ is single-valued with a finite number of discontinuities in $[-\pi, \pi]$.
2. $f(t)$ has a finite number of extrema in $[-\pi, \pi]$.
3. The absolute value of $f(t)$ is integrable in $[-\pi, \pi]$ such that $\int_0^\pi |f(t)|\mathrm{d}t$ exists.
4. $f(t)$ is 2π-periodic.

Suppose that $f(t)$ satisfies the conditions; the CFS representation is given by

$$f(t) = \sum_{k=-\infty}^{\infty} b_k e^{ikt} \quad \text{with} \quad b_k = \frac{1}{2\pi} \int_{-\pi}^{+\pi} f(t) e^{-ikt} dt. \tag{6}$$

Now, if we extend the series to support any real function on a finite interval $[a, b]$ and satisfying the Dirichlet conditions, the complex Fourier series expansion can be defined:

$$f(x) = \mathfrak{Re}\left(\sum_{k=-\infty}^{\infty} b_k e^{i\frac{2\pi}{b-a}kx} \right) \text{ with } b_k = \frac{1}{b-a} \int_a^b f(x) e^{-i\frac{2\pi}{b-a}kx} dx. \tag{7}$$

If we truncate the summation and allow a summation truncation error, we have

$$f(x) \approx f_k(x) = \mathfrak{Re}\left(\sum_{k=-N}^{N} b_k e^{i\frac{2\pi}{b-a}kx} \right). \tag{8}$$

Finally, as $f(x)$ is a real function, Equation (8) becomes

$$f_k(x) = \mathfrak{Re}\left(2\sum_{k=0}^{N} b_k e^{i\frac{2\pi}{b-a}kx} - b_0 \right). \tag{9}$$

As we see in the next section, we use Equation (9) to represent the option prices on a finite interval $[a, b]$. It is clear that the general option prices, either on a forward (futures) or not, are continuous,

have a finite number of extrema and must be integrable in a finite interval. Moreover, as the option prices are truncated in a finite interval, we assume accordingly that the option prices are also periodic.

3. Truncated Intervals and Complex Fourier Series Expression of European Option Prices

In this section, we derive closed-form formulae for European-style options using the CFS method. We first assume an incomplete market consisting of one risky asset $\{S_t\}_{t\geq 0}$ (notable exceptions are when the Lévy process is Brownian motion–the classical Black and Scholes model–or a Poisson process) with a continuous dividend at a constant rate q and a risk-free rate r. As this is an incomplete market (cf. Cont and Tankov, 2004), there exist infinitely many equivalent martingale measures Q under which prices of derivative assets are equal to discounted expectations of future payoffs. We assume that the market has already chosen one of the possible risk-neutral measures, and expectations $\mathbb{E}$ will always be taken with respect to this chosen measure. Under this risk-neutral measure, the asset price process evolves as

$$\mathbb{E}[S_T] = \mathbb{E}\left[S_t e^{L_T - L_t}\right] = S_t e^{(r-q)(T-t)}. \tag{10}$$

where $L_T - L_t$ is either a Lévy process or an affine stochastic volatility process. If we have a European option (an option that is exercised only at maturity), the underlying asset of which is driven by $\{S_t\}_{t\geq 0}$, and the current log-price $x := \log S_t$, we can express the option price $V(x,t)$ at time t with its contingent claim paying out $G(S_T)$ at maturity $T \geq t$ as follows:

$$V(x,t) = e^{-r(T-t)}\mathbb{E}\left[G(S_T)|S_t = e^x\right] = e^{-r(T-t)}\int_{-\infty}^{+\infty} G(e^{x+z})f(z)dz, \tag{11}$$

where $z \in L_T - L_t$. Furthermore, if we choose an interval $[a,b]$ satisfying Equation (2) and use a change of variables and setting $y = x + z$ and $\mathrm{d}y = \mathrm{d}x$, we transform Equation (11) into a new formula such that

$$V(x,t) \approx e^{-r(T-t)}\int_a^b G(e^y)f(y-x)dy. \tag{12}$$

Before we show the CFS pricing formula of any European-type option, we show how to choose a good truncated interval to ensure that the equality (2) can hold while the CFS pricing formula can remain accurate. The performance of the CFS method is indeed sensitive to the choice of the truncated interval. If the interval's size is fairly small, then the resulting option prices will be inaccurate. Conversely, if the interval is too large, more terms are required in the series expansions to reach a certain degree of accuracy. Hence, to ensure high accuracy of option prices for a reasonable size of a truncated interval $[a,b]$, we adopt and modify the ideas suggested by Fang and Oosterlee

(2009) to create $[a, b]$. In brief, Fang and Oosterlee (2009) proposed to use the following formulas:

$$[a,b] = \left[(c_1 + x_t) - L\sqrt{c_2 + \sqrt{c_4}},\ (c_1 + x_t) + L\sqrt{c_2 + \sqrt{c_4}}\right].$$

Here, c_1, c_2, and c_4 are the first, second and fourth stochastic process cumulants respectively, L is any constant number chosen from $[10, 12]$, and $x_t := \log(S_t/K)$ if S_t represents the risky asset price driven by the same stochastic process at t and K is short for the strike price. Their idea is clearly excellent, but to obtain a better truncated interval to fit in the CFS framework, we improve on their approach and propose Algorithm 1. If at t, S_t stands for the risky asset price again, F^{fwd} denotes the forward price, and F^{fut} stands for the futures price, we construct a formula of $\mathbf{D}$ that is the value of $\log(S_t/K)$, $\log(F_t^{fwd}/K)$ or $\log(F_t^{fut}/K)$ such that, by trial and error,

$$\begin{aligned} b &= |c_1 + L\sqrt{c_2 + \sqrt{c_4}} + |\mathbf{D}|| \\ a &= -b \end{aligned} \tag{13}$$

Algorithm 1: Truncated interval

The closed-form formulas for c_1, c_2, and c_4 are shown in Table B.18 in Appendix B. However, in the Heston model (cf. Appendix A), we use an absolute value of c_2 and ignore the value of c_4 due to the negative value of c_2 and the lengthy representation of c_4 (cf. Fang and Oosterlee, 2008). We therefore have $c_1 + L\sqrt{|c_2|}$ rather than $c_1 + L\sqrt{c_2 + \sqrt{c_4}}$ in Algorithm 1.

Once we have a truncated interval, we can turn our attention to formulating our CFS pricing formulae for different European-type options.

Theorem 1. *When a dividend-paying risky asset price process $(S_t)_{t\geq 0}$ with an analytical characteristic function $\phi(\cdot)$ has a current asset price of $e^x = S$, risk-free interest rate r and compounded continuous dividend q, a complex Fourier expansion pricing formula of a* ***European-type option*** *driven by this process with maturity time T and strike price K is*

$$V(x,t) = e^{-r(T-t)-\zeta x}\mathfrak{Re}\left(2\sum_{k=1}^{N}\widehat{B}_k e^{i\frac{2\pi}{b-a}kx} + \widehat{B}_0\right) \tag{14}$$

with

$$\widehat{B}_k = \tfrac{1}{b-a}\widehat{G}\left(-\tfrac{2\pi k}{(b-a)} - \zeta i\right)\phi\left(\tfrac{2\pi k}{(b-a)} + \zeta i\right), \quad \widehat{B}_0 = \tfrac{1}{b-a}\widehat{G}\left(-\zeta i\right)\phi\left(\zeta i\right), \tag{15}$$

where $[a, b]$ satisfies the condition (2), ζ is a damping factor and $\widehat{G}(\cdot)$ is the Fourier transform of the payoff function.

Proof: We first multiply a damping factor $\exp(\zeta x)$, where ζ is any number of $\mathbb{R}$ but not equal to

zero, by $V(x,t)$ to obtain a product of $U(x,t)$ such that

$$e^{\zeta x}V(x,t) = U(x,t). \tag{16}$$

Then, we express $U(x,t)$ with a CFS expansion defined as

$$U(x,t) = 2\sum_{k=0}^{N} \widehat{U}_k e^{i\frac{2\pi}{b-a}kx} - \widehat{U}_0 \tag{17}$$

$$= 2\sum_{k=1}^{N} \widehat{U}_k e^{i\frac{2\pi}{b-a}kx} + \widehat{U}_0 \tag{18}$$

with

$$\widehat{U}_k = \frac{1}{b-a}\int_a^b U(x,t)e^{-i\frac{2\pi}{b-a}kx}dx = \frac{1}{b-a}\int_a^b V(x,t)e^{-i\left(\frac{2\pi}{b-a}k+\zeta i\right)x}dx. \tag{19}$$

To seek the closed-form Fourier expression of $\widehat{U}_k$, we define $\widetilde{\omega}_k = \frac{2\pi}{b-a}k + \zeta i$, $y - x = \chi$ and $\mathrm{d}\chi = \mathrm{d}x$. Then, based on the result of (12), we have

$$\widehat{U}_k \approx e^{-r(T-t)}\frac{1}{b-a}\int_a^b\int_a^b G(e^y)f(y-x)e^{-i\widetilde{\omega}_k(x)}dydx \tag{20}$$

$$\approx e^{-r(T-t)}\frac{1}{b-a}\int_a^b\int_a^b G(e^y)f(\chi)e^{-i\widetilde{\omega}_k(y-\chi)}dyd\chi. \tag{21}$$

Since $\int_a^b f(\chi)e^{i\widetilde{\omega}_k\chi}d\chi \approx \phi(\widetilde{\omega}_k)$ (cf. Equation (2)), denoting $\int_a^b G(e^y)e^{-i\widetilde{\omega}_k y}dy$ as $\widehat{G}(-\widetilde{\omega}_k)$, we can further infer that

$$\widehat{U}_k = e^{-r(T-t)}\frac{1}{b-a}\int_a^b G(e^y)e^{-i\widetilde{\omega}_k y}dy\int_a^b f(\chi)e^{i\widetilde{\omega}_k\chi}d\chi \tag{22}$$

$$\approx e^{-r(T-t)}\frac{1}{b-a}\widehat{G}(-\widetilde{\omega}_k)\phi(\widetilde{\omega}_k) \tag{23}$$

$$= e^{-r(T-t)}\frac{1}{b-a}\widehat{G}\left(-\frac{2\pi}{b-a}k-\zeta i\right)\phi\left(\frac{2\pi}{b-a}k+\zeta i\right) \tag{24}$$

Based on the result above, if we express $\widehat{U}$ with the form of Equation (18) to maintain fewer exponential function terms, we can see that

$$U(x,t) = 2\sum_{k=1}^{N} \widehat{U}_k e^{i\frac{2\pi}{b-a}kx} + \widehat{U}_0 \tag{25}$$

$$= e^{-r(T-t)}\left(2\sum_{k=1}^{N}\frac{1}{b-a}\widehat{G}\left(-\widetilde{\omega}_k\right)\phi\left(\widetilde{\omega}_k\right)e^{i\frac{2\pi}{b-a}kx} + \frac{1}{b-a}\widehat{G}(-\widetilde{\omega}_0)\phi(\widetilde{\omega}_0)\right) \tag{26}$$

$$= e^{-r(T-t)}\left(2\sum_{k=1}^{N}\frac{1}{b-a}\widehat{G}\left(-\frac{2\pi}{b-a}k-\zeta i\right)\phi\left(\frac{2\pi}{b-a}k+\zeta i\right)e^{i\frac{2\pi}{b-a}kx}\right.$$
$$\left.+\frac{1}{b-a}\widehat{G}(-\zeta i)\phi(\zeta i)\right). \tag{27}$$

Finally, as $V(x,t)$ is a real function, we denote $\widehat{B}(\cdot)$ as $1/(b-a)\widehat{G}(\cdot)\phi(\cdot)$ and divide $U(x,t)$ by $\exp(\zeta x)$, and accordingly, the complex Fourier option pricing formula becomes

$$V(x,t) = e^{-r(T-t)-\zeta x}\mathfrak{Re}\left(2\sum_{k=1}^{N}\widehat{B}_k e^{i\frac{2\pi}{b-a}kx}+\widehat{B}_0\right) \tag{28}$$

with

$$\widehat{B}_k = \tfrac{1}{b-a}\widehat{G}\left(-\tfrac{2\pi k}{b-a}-\zeta i\right)\phi\left(\tfrac{2\pi k}{b-a}+\zeta i\right), \quad \widehat{B}_0 = \tfrac{1}{b-a}\widehat{G}\left(-\zeta i\right)\phi\left(\zeta i\right). \tag{29}$$

Q. E. D.

Remark 2. $\exp(\zeta x)$ *is a damping factor that acts like the one introduced in Carr and Madan (1991). Moreover, it cannot be equal to zero because if it is,* $\widehat{G}$ *does not exist when* $k = 0$*. By trial and error, the value of* ζ *is chosen as* 0.5.

Apart from a chooser option, Theorem 1 can be applied to any options that have payoff functions listed in Table 1. As a chooser option contract allows the holder to decide whether it is a call or put prior to the expiration date, its CFS pricing formula is slightly different from Equation (14). Nevertheless, we can still adopt the idea of Theorem 1 to derive the formula.

Corollary 3. *A* ***European chooser option*** *with exercise time* $T_c < T$ *allows the holder to choose, at time* T_c*, between a put of* $P(x,T_c)$ *and a call of* $C(x,T_c)$ *with identical maturity* T *and strike* K*. Its payoff at* T *is therefore* $\max\left(P(x,T_c),C(x,T_c)\right)$*. A CFS pricing formula of this option can be expressed as follows:*

$$V_{\text{Chooser}}(x,t) = P(x,t) + C(x,t) \tag{30}$$

where

$$P(x,t) = e^{-r(T-t)-\zeta x}\mathfrak{Re}\left(2\sum_{k=1}^{N}\widehat{B}_k e^{i\frac{2\pi}{b-a}kx}+\widehat{B}_0\right)$$

and

$$C(x,t) = e^{-r(T_c-t)-\zeta x}\mathfrak{Re}\left(2\sum_{k=1}^{N}\widehat{B}_{1,k} e^{i\frac{2\pi}{b-a}kx}+\widehat{B}_{1,0}\right)$$

with

$$\widehat{B}_k = \tfrac{1}{b-a}\widehat{G}\left(-\tfrac{2\pi k}{b-a}-\zeta i\right)\phi\left(\tfrac{2\pi k}{b-a}+\zeta i\right), \quad \widehat{B}_0 = \tfrac{1}{b-a}\widehat{G}\left(-\zeta i\right)\phi\left(\zeta i\right) \tag{31}$$

Table 1: Complex Fourier transforms for a variety of financial contingency claims.

Financial Contingency Claim	Payoff Function	Fourier Transform
	$G(e^y)$ or $G_1(e^y)$	$\int_a^b G(e^y)e^{-i\widetilde{\omega}_k y}dy$ or $\int_a^b G_1(e^y)e^{-i\widetilde{\omega}_k y}dy$
Call	$(e^y - K)^+$	$Ke^{-i\widetilde{\omega}_k(\log K)}\left(\frac{e^{(1-i\widetilde{\omega}_k)b}-1}{1-i\widetilde{\omega}_k} - \frac{e^{i\widetilde{\omega}_k b}-1}{i\widetilde{\omega}_k}\right)$
Put	$(K - e^y)^+$	$-Ke^{-i\widetilde{\omega}_k(\log K)}\left(\frac{e^{(1-i\widetilde{\omega}_k)a}-1}{1-i\widetilde{\omega}_k} - \frac{e^{i\widetilde{\omega}_k a}-1}{i\widetilde{\omega}_k}\right)$
Covered Call	$\min(e^y, K)$	$Ke^{-i\widetilde{\omega}_k(\log K)}\left(\frac{e^{(1-i\widetilde{\omega}_k)a}-1}{1-i\widetilde{\omega}_k} - \frac{e^{i\widetilde{\omega}_k a}-1}{i\widetilde{\omega}_k}\right)$
Cash-or-Nothing Call	$\mathbb{1}_{e^y \geq K}$	$e^{-i\widetilde{\omega}_k(\log K)}\left(\frac{e^{i\widetilde{\omega}_k b}-1}{i\widetilde{\omega}_k}\right)$
Cash-or-Nothing Put	$\mathbb{1}_{e^y \leq K}$	$-e^{-i\widetilde{\omega}_k(\log K)}\left(\frac{e^{i\widetilde{\omega}_k a}-1}{i\widetilde{\omega}_k}\right)$
Asset-or-Nothing Call	$e^y\mathbb{1}_{e^y \geq K}$	$e^{-i\widetilde{\omega}_k(\log K)}\left(\frac{e^{(1-i\widetilde{\omega}_k)b}-1}{1-i\widetilde{\omega}_k}\right)$
Asset-or-Nothing Put	$e^y\mathbb{1}_{e^y \leq K}$	$-e^{-i\widetilde{\omega}_k(\log K)}\left(\frac{e^{(1-i\widetilde{\omega}_k)a}-1}{1-i\widetilde{\omega}_k}\right)$
Asymmetric Call	$(e^{ny} - K^n)\mathbb{1}_{e^y \geq K}$	$K^n e^{-i\widetilde{\omega}_k(\log K)}\left(\frac{e^{(n-i\widetilde{\omega}_k)b}-1}{n-i\widetilde{\omega}_k} - \frac{e^{i\widetilde{\omega}_k b}-1}{i\widetilde{\omega}_k}\right)$
Asymmetric Put	$(K^n - e^{ny})\mathbb{1}_{e^y \leq K}$	$-K^n e^{-i\widetilde{\omega}_k(\log K)}\left(\frac{e^{(n-i\widetilde{\omega}_k)a}-1}{n-i\widetilde{\omega}_k} - \frac{e^{i\widetilde{\omega}_k a}-1}{i\widetilde{\omega}_k}\right)$
Symmetric Call	$(e^y - K)^n\mathbb{1}_{e^y \geq K}$	$e^{-i\widetilde{\omega}_k(\log K)}\sum_{j=0}^{n}\binom{n}{j}(-K)^{n-j}\left(\frac{e^{(j-i\widetilde{\omega}_k)b}-1}{j-i\widetilde{\omega}_k}\right)$
Symmetric Put	$(K - e^y)^n\mathbb{1}_{e^y \leq K}$	$-e^{-i\widetilde{\omega}_k(\log K)}\sum_{j=0}^{n}\binom{n}{j}(K)^j(-1)^{n-j}\left(\frac{e^{(n-j-i\widetilde{\omega}_k)a}-1}{n-j-i\widetilde{\omega}_k}\right)$
Chooser Call	$(e^{y-q(T-T_c)} - Ke^{-r(T-T_c)})^+$	$Ke^{-r(T-T_c)}e^{-i\widetilde{\omega}_k\widetilde{K}}\left(\frac{e^{(1-i\widetilde{\omega}_k)b}-1}{1-i\widetilde{\omega}_k} - \frac{e^{i\widetilde{\omega}_k b}-1}{i\widetilde{\omega}_k}\right)$, where $\widetilde{K} = \log K - (r-q)(T-T_c)$

and

$$\widehat{B}_{1,k} = \tfrac{1}{b-a}\widehat{G}_1\left(-\tfrac{2\pi k}{b-a} - \zeta i\right)\phi\left(\tfrac{2\pi k}{b-a} + \zeta i\right), \quad \widehat{B}_{1,0} = \tfrac{1}{b-a}\widehat{G}_1\left(-\zeta i\right)\phi\left(\zeta i\right). \tag{32}$$

Proof: By using the put-call parity $C(x,T_c) + Ke^{-r(T-T_c)} = P(x,T_c) + S_{T_c}e^{-q(T-T_c)}$ at T_c, we can easily see that the payoff of a chooser option at T_c is

$$\max\left(C(x,T_c), P(x,T_c)\right) = P(x,T_c) + \max\left(S_{T_c}e^{-q(T-T_c)} - e^{-r(T-T_c)}K, 0\right).$$

To determine the first put option at time t, we take discounted risk-neutral expectations of the payoff and make use of the fact that $e^{-r(T_c-t)}\mathbb{E}\left(P(x,T_c)\right) = P(x,t)$. Using the CFS approximation scheme, $P(x,t)$ is given by

$$P(x,t) = \quad e^{-r(T-t)-\zeta x}\mathfrak{Re}\left(2\sum_{k=1}^{N}\widehat{B}_k e^{i\frac{2\pi}{b-a}kx} + \widehat{B}_0\right) \tag{33}$$

Here, $\widehat{B}_k$ and $\widehat{B}_0$ are defined as Equation (29) in Theorem 1. For the call price, we have to take into account that the call is exercised at time T_c with strike $e^{-r(T-T_c)}K$. Hence,

$$C(x,t) = \quad e^{-r(T_c-t)-\zeta x}\mathfrak{Re}\left(2\sum_{k=1}^{N}\widehat{B}_{1,k} e^{i\frac{2\pi}{b-a}kx} + \widehat{B}_{1,0}\right) \tag{34}$$

with

$$\widehat{B}_{1,k} = \tfrac{1}{b-a}\widehat{G}_1\left(-\tfrac{2\pi k}{b-a} - \zeta i\right)\phi\left(\tfrac{2\pi k}{b-a} + \zeta i\right), \quad \widehat{B}_{1,0} = \tfrac{1}{b-a}\widehat{G}_1\left(-\zeta i\right)\phi\left(\zeta i\right). \tag{35}$$

We express $\widehat{G}_1(\cdot)$ in detail in the next section. In Equation (35), the time variable (time-to-maturity) in $\phi(\cdot)$ should be set to $T_c - t$. Finally, by combining the results of $P(t,x)$ and $C(t,x)$, the result of Equation (30) follows. Q. E. D.

Given the simplicity of Equation (14), it is easy to price an option on a forward contract with the current forward price F_t^{fwd}. In general, the key idea is to use the spot price-forward relationship:

$$\begin{aligned} F_t^{fwd} &= S_t e^{(r-q)(T-t)} \\ F^{fwd} &= Se^{(r-q)(T-t)}. \end{aligned} \tag{36}$$

As a function of the log-forward $\hat{x} := \log(F^{fwd})$, we can further simplify the equation to

$$x = \frac{\hat{x}}{(r-q)(T-t)}. \tag{37}$$

Corollary 4. *For a **European option on a forward contract** with the same conditions as in*

Theorem 1 *and* F *and* S *equal to* $\exp(\hat{x})$ *and* $\exp(x)$*, respectively, the CFS pricing formula is*

$$V_{\text{fwd}}(\hat{x},t) = \quad e^{-r(T-t)-\frac{\zeta}{(r-q)(T-t)}\hat{x}}\mathfrak{Re}\left(2\sum_{k=1}^{N}\widehat{B}_k e^{i\frac{2\pi}{(b-a)(r-q)(T-t)}k\hat{x}}+\widehat{B}_0\right) \tag{38}$$

with

$$\widehat{B}_k = \frac{1}{b-a}\widehat{G}\left(-\frac{2\pi k}{b-a}-\zeta i\right)\phi\left(\frac{2\pi k}{b-a}+\zeta i\right), \qquad \widehat{B}_0 = \frac{1}{b-a}\widehat{G}\left(-\zeta i\right)\phi\left(\zeta i\right), \tag{39}$$

$$\widehat{G}\left(-\frac{2\pi k}{b-a}-\zeta i\right) = \int_a^b G(e^y)e^{-i\left(\frac{2\pi k}{b-a}+\zeta i\right)y}dy, \qquad \widehat{G}\left(-\zeta i\right) = \int_a^b G(e^y)e^{-i(\zeta i)y}dy. \tag{40}$$

Proof: To prove the corollary, we substitute Equation (37) into Equation (14), and Equation (38) and Equation (39) will follow. Q. E. D.

Based on Equation (38) and Equation (39), it is straightforward to derive a formula for a call/put on futures prices. Therefore, we have the following corollary:

Corollary 5. ***A European option on a futures contract****. Suppose that there is a constant risk-free interest rate* r *and a log futures price* $\log(F^{fut}) = \overline{x}$ *of a particular underlying that has a traceable characteristic function. Then, a CFS pricing formula states the price for a European call option of maturity* T *on a futures contract with strike price* K *and delivery date* T' *(with* $T' \geq T$*) as follows:*

$$V_{\text{fut}}(\hat{x},t) = \quad e^{-r(T-t)-\zeta\overline{x}}\mathfrak{Re}\left(2\sum_{k=1}^{N}\widehat{B}_k e^{i\frac{2\pi}{b-a}k\overline{x}}+\widehat{B}_0\right) \tag{41}$$

with

$$\widehat{B}_k = \frac{1}{b-a}\widehat{G}\left(-\frac{2\pi k}{b-a}-\zeta i\right)\phi\left(\frac{2\pi k}{b-a}+\zeta i\right), \qquad \widehat{B}_0 = \frac{1}{b-a}\widehat{G}\left(-\zeta i\right)\phi\left(\zeta i\right), \tag{42}$$

$$\widehat{G}\left(-\frac{2\pi k}{b-a}-\zeta i\right) = \int_a^b G(e^y)e^{-i\left(\frac{2\pi k}{b-a}+\zeta i\right)y}dy, \qquad \widehat{G}\left(-\zeta i\right) = \int_a^b G(e^y)e^{-i(\zeta i)y}dy. \tag{43}$$

Proof: As in Equation (36), we first exploit the fact that the futures price F^{fut} starting at t with delivery date T' is given by $F^{fut} = S$ and $r = q$. Then, considering both $\log(F^{fut}) = \overline{x}$ and $\log S = x$, we replace x with $\overline{x}$ in both Equation (14) and Equation (29). We can therefore formulate Equation (41) and Equation (42). Q. E. D.

Note that T' does not appear in the formulae even though it could be greater than T. This is because futures contracts are marked to market, and thus the payoff is realised when the option is exercised.

4. Complex Fourier Series Expression of Payoff Functions and Greeks Derivation

In this section, we demonstrate some essential algebraic steps of the Fourier transform of payoff functions $\widehat{G}(-\widetilde{\omega}_k) = \int_a^b e^{-i\widetilde{\omega}_k y}G(e^y)\mathrm{d}y$ in Equation (23). As we define $G(e^y)$ in a finite interval

220 $[a,b]$ rather than $[-\infty,\infty]$, $\widehat{G}(-\widetilde{\omega}_k)$ accordingly exists in $\mathbf{L}_1$[1] space. If we use a vanilla call payoff function as a sample to derive its Fourier transform, the algebraic steps are as follows:

$$\begin{aligned}\widehat{G}(-\widetilde{\omega}_k) &= \int_a^b e^{-i\widetilde{\omega}_k y}(e^y - K)^+ \mathrm{d}y \\ &= K\int_0^{b-\log K} e^{-i\widetilde{\omega}_k(y+\log K)}(e^y - 1)\mathrm{d}y \\ &= Ke^{-i\widetilde{\omega}_k(\log K)}\left(\frac{e^{(1-i\widetilde{\omega}_k)(b-\log K)}-1}{1-i\widetilde{\omega}_k} + \frac{e^{-i\widetilde{\omega}_k(b-\log K)}-1}{i\widetilde{\omega}_k}\right) \end{aligned} \tag{44}$$

In the integral, we replace the upper limit $b - \log K$ with b, as we define b in Algorithm 1, which is larger or equal to $b - \log K$, later in this section. Hence, $\widehat{G}(-\widetilde{\omega}_k)$ can be rewritten as

$$Ke^{-i\widetilde{\omega}_k \log K}\left(\frac{e^{(1-i\widetilde{\omega}_k)b}-1}{1-i\widetilde{\omega}_k} + \frac{e^{-i\widetilde{\omega}_k b}-1}{i\widetilde{\omega}_k}\right).$$

Applying the same idea, the $\widehat{G}(-\widetilde{\omega}_k)$ of a vanilla put payoff is

$$-Ke^{-i\widetilde{\omega}_k \log K}\left(\frac{e^{(1-i\widetilde{\omega}_k)a}-1}{1-i\widetilde{\omega}_k} - \frac{e^{i\widetilde{\omega}_k a}-1}{i\widetilde{\omega}_k}\right).$$

Note that $\widehat{G}(-\widetilde{\omega}_k)$ exists because $|\widetilde{\omega}_k| = |\frac{2\pi}{b-a}k + \zeta i|$, where ζ is any number of $\mathbb{R}$ but not equal to zero. This explains why we multiply the factor $\exp(\zeta x)$ by $V(x,t)$ in Equation (16), as we can guarantee the existence of $\widehat{G}(\widetilde{\omega}_k)$. Applying the steps above, we are able to derive the Fourier transform of different option payoffs. The results are shown in Table 1. As the call price $C(x,T_c)$ in the chooser option is exercised at time T_c with strike $e^{-r(T-T_c)}K$, it is worth mentioning the derivation of the algebraic steps of $\widehat{G}_1(\cdot)$ in Equation (34). If we first set $\widetilde{K} = \log K - (r-q)(T-T_c)$, then we have

$$\begin{aligned}\widehat{G}_1(-\widetilde{\omega}_k) &= \int_a^b e^{-i\widetilde{\omega}_k y}(e^{y-q(T-T_c)} - Ke^{-r(T-T_c)})^+ \mathrm{d}x \\ &\approx Ke^{-r(T-T_c)}e^{-i\widetilde{\omega}_k \widetilde{K}}\left(\frac{e^{(1-i\widetilde{\omega}_k)b}-1}{1-i\widetilde{\omega}_k} + \frac{e^{-i\widetilde{\omega}_k b}-1}{i\widetilde{\omega}_k}\right) \end{aligned} \tag{45}$$

If we consider options on a forward (futures) contract, the general forms of $\widehat{G}$ and $\widehat{G}_1$ are the same as those shown in Table 1 but with slightly different values of $[a,b]$. The choice of $[a,b]$ will be

[1] In mathematics, L_1 spaces are function spaces defined using the 1-norm $\|\mathbf{x}\| = \sum_{i=1}^N |x_i|$, where $\mathbf{x}$ is a vector, for finite-dimensional vector spaces, which are sometimes called Lebesgue spaces.

discussed later in this section.

Now, we turn our attention to deriving option Greeks. Although accurately valuing financial claims plays a key role in financial modelling, the risk management (hedging) of these derivative instruments is equally important. Financial institutions manage option risk when they sell options to their clients through the analysis of "Greek letters". Greek letters are defined as the sensitivities of the option price to a single-unit change in the value of either a state variable or a parameter. Such sensitivities can represent the different dimensions of the risk associated with an option. In this paper, we focus only on deriving Delta, Δ, the rate of change in the option value with respect to changes in the underlying asset's price, and Gamma, Γ, the rate of change in Delta with respect to changes in the underlying price. Other Greeks, such as Theta, can be derived in a similar fashion; however, depending on the particular characteristic function, the derivation expression might be rather lengthy. We omit them here, as many terms are repeated.

Delta is the first derivative of the value $V(x,t)$ of the option with respect to the underlying instrument's price S. Hence, differentiating Equation (14) with respect to S, we have

$$\begin{aligned}\Delta_t = \frac{\partial V(x,t)}{\partial S} &= \frac{\partial V(x,t)}{\partial x}\frac{\partial x}{\partial S} \\ &= e^{-r(T-t)}\mathfrak{Re}\left(2\sum_{k=1}^{N}\left(i\frac{2\pi}{b-a}k-\zeta\right)\widehat{B}_k e^{(i\frac{2\pi}{b-a}k-\zeta-1)x}\right. \\ &\qquad \left. -\zeta\widehat{B}_0 e^{-(\zeta+1)x}\right). \end{aligned} \tag{46}$$

In a similar fashion, we can obtain Γ_t by differentiating Δ_t with respect to S again, such that

$$\Gamma_t = \frac{\partial^2 V(x,t)}{\partial S^2} = \frac{\partial \Delta_t}{\partial S} = \frac{\partial \Delta_t}{\partial x}\frac{\partial x}{\partial S}. \tag{47}$$

Hence,

$$\begin{aligned}\Gamma_t = e^{-r(T-t)}\mathfrak{Re}\left(2\sum_{k=1}^{N}\left(i\frac{2\pi}{b-a}k-\zeta-1\right)\left(i\frac{2\pi}{b-a}k-\zeta\right)\widehat{B}_k e^{(i\frac{2\pi}{b-a}k-\zeta-2)x}\right. \\ \left. +(\zeta+1)\zeta\widehat{B}_0 e^{-(\zeta+2)x}\right). \end{aligned} \tag{48}$$

Based on the above formulas, the Delta $\Delta_t^{fwd}(\Delta_t^{fut})$ and Gamma $\Gamma_t^{fwd}(\Gamma_t^{fut})$ of options on a forward (futures) contract are as follows:

$$\Delta_t^{fwd} = e^{-r(T-t)}\mathfrak{Re}\left(2\sum_{k=1}^{N}\frac{1}{(r-q)(T-t)}\left(i\frac{2\pi}{b-a}k-\zeta\right)\widehat{B}_k e^{\left(i\frac{2\pi}{(r-q)(T-t)(b-a)}k-\frac{\zeta}{(r-q)(T-t)}-1\right)\hat{x}}\right.$$

$$- \frac{\zeta}{(r-q)(T-t)} \widehat{B}_0 e^{-\left(\frac{\zeta}{(r-q)(T-t)}+1\right)\hat{x}} \Bigg). \tag{49}$$

$$\Delta_t^{fut} = e^{-r(T-t)} \mathfrak{Re}\left(2\sum_{k=1}^{N} \left(i\frac{2\pi}{b-a}k - \zeta \right) \widehat{B}_k e^{(i\frac{2\pi}{b-a}k-\zeta-1)\overline{x}} - \zeta \widehat{B}_0 e^{-(\zeta+1)\overline{x}} \right). \tag{50}$$

$$\begin{aligned} \Gamma_t^{fwd} = e^{-r(T-t)} \mathfrak{Re}\Bigg(2\sum_{k=1}^{N} & \left(i\frac{2\pi}{(r-q)(T-t)(b-a)}k - \frac{\zeta}{(r-q)(T-t)} - 1 \right) \frac{1}{(r-q)(T-t)} \left(i\frac{2\pi}{b-a}k - \zeta \right) \\ & \times \widehat{B}_k e^{\left(i\frac{2\pi}{(r-q)(T-t)(b-a)}k - \frac{\zeta}{(r-q)(T-t)} - 2\right)\hat{x}} \\ & - \left(\frac{\zeta}{(r-q)(T-t)} - 1 \right) \frac{\zeta}{(r-q)(T-t)} \widehat{B}_0 e^{-\left(\frac{\zeta}{(r-q)(T-t)}+2\right)\hat{x}} \Bigg). \end{aligned} \tag{51}$$

$$\begin{aligned} \Gamma_t^{fut} = e^{-r(T-t)} \mathfrak{Re}\Bigg(2\sum_{k=1}^{N} & \left(i\frac{2\pi}{b-a}k - \zeta - 1 \right) \left(i\frac{2\pi}{b-a}k - \zeta \right) \widehat{B}_k e^{(i\frac{2\pi}{b-a}k-\zeta-2)\overline{x}} \\ & + (\zeta+1)\zeta \widehat{B}_0 e^{-(\zeta+2)\overline{x}} \Bigg). \end{aligned} \tag{52}$$

It is also easy to obtain the formula for Vega, $\frac{\partial V}{\partial y_t}$, where y_t is the initial value of the volatility at time t. For example, for the Heston model, as y_0 is the initial value of the volatility in (A.25), we derive Vega as follows:

$$\frac{\partial V(x, y_0, t)}{\partial y_0} = e^{-r(T-t)-\zeta x} \left(\mathfrak{Re}\left[2\sum_{k=1}^{\infty} \frac{\partial \widehat{B}_k}{\partial y_0} e^{i\frac{2\pi}{b-a}kx} + \frac{\partial \widehat{B}_0}{\partial y_0} \right] \right), \tag{53}$$

with

$$\frac{\partial \widehat{B}_k}{\partial y_0} = \frac{1}{b-a} \widehat{G}\left(-\frac{2\pi k}{b-a} - \zeta i \right) \frac{\partial \phi\left(\frac{2\pi k}{b-a} + \zeta i, y_0 \right)}{\partial y_0}, \; \frac{\partial \widehat{B}_0}{\partial y_0} = \frac{1}{b-a} \widehat{G}\left(-\zeta i \right) \frac{\partial \phi\left(\zeta i, y_0 \right)}{\partial y_0}, \tag{54}$$

where ϕ contains the parameter y_0.

5. Error Analysis

In this section, we demonstrate that the total error from pricing European-type options can be made very small by choosing a suitably large interval $[a, b]$. As long as a PDF is supported on $[a, b]$ and is everywhere smooth[2] except at a point that has discontinuity in one of its derivatives, the exponential convergence rate is guaranteed in the complex Fourier expansions.

Before we launch our error analysis, we standardise the mathematical notations to make the

[2]We say that a PDF is everywhere smooth if $f(x) \subset C^{\infty}[a, b]$, where $C^{\infty}$is an infinitely differentiable space and $[a, b] \in \mathbb{R}$.

analysis more comprehensible. In section 3, the CFS pricing formula for European options can be written as the following two interchangeable formulas:

$$V(x,t) = \quad e^{-r(T-t)-\zeta x}\mathfrak{Re}\left(2\sum_{k=1}^{N}\widehat{B}_k e^{i\frac{2\pi}{b-a}kx}+\widehat{B}_0\right) \tag{55}$$

or

$$V(x,t) = \quad e^{-r(T-t)-\zeta x}\mathfrak{Re}\left(2\sum_{k=0}^{N}\widehat{B}_k e^{i\frac{2\pi}{b-a}kx}-\widehat{B}_0\right), \tag{56}$$

with

$$\widehat{B}_k = \frac{1}{b-a}\widehat{G}\left(-\widetilde{\omega}_k\right)\phi\left(\widetilde{\omega}_k\right),\ \widehat{B}_0 = \frac{1}{b-a}\widehat{G}\left(-\widetilde{\omega}_0\right)\phi\left(\widetilde{\omega}_0\right),\ \widetilde{\omega}_k = \frac{2\pi k}{(b-a)}+\zeta i. \tag{57}$$

When we derive the CFS pricing formulas in Section 3, we use the forms of Equation (55), as we wish to reduce the number of the $e^{i\frac{2\pi}{b-a}kz}$ terms appearing in the formulas. However, ultimately, in the error analysis, we instead use Equation (56) for comprehensibility.

There are three types of approximation errors in any call/put option in this paper.

1. The integration truncation error:

$$\epsilon_1 := \left|\left(\int_{-\infty}^{+\infty}G(e^{z+x})f(z)\mathrm{d}z-\int_a^b G(e^{z+x})f(z)\mathrm{d}z\right)\right| \tag{58}$$

2. The error related to approximating $\frac{1}{b-a}\int_a^b G(e^y)e^{-i\widetilde{\omega}_k y}\mathrm{d}y\int_a^b f(z)e^{i\widetilde{\omega}_k z}dz$ in (22) with $\widehat{B}_k = \frac{1}{b-a}\widehat{G}\left(-\widetilde{\omega}_k\right)\phi\left(\widetilde{\omega}_k\right)$ in (23):

$$\begin{aligned}\epsilon_2 := \Bigg|e^{\zeta x}\Bigg(2\sum_{k=0}^{N}\left(\frac{1}{b-a}\int_a^b G(e^y)e^{-i\widetilde{\omega}_k y}\mathrm{d}y\int_a^b f(z)e^{i\widetilde{\omega}_k z}\mathrm{d}z\right)e^{i\frac{2\pi}{b-a}kx}- \\ \frac{1}{b-a}\int_a^b G(e^y)e^{-i\widetilde{\omega}_0 y}\mathrm{d}y\int_a^b f(z)e^{i\widetilde{\omega}_0 z}\mathrm{d}z\Bigg)-\left(e^{\zeta x}\left(2\sum_{k=0}^{N}\widehat{B}_k e^{i\frac{2\pi}{b-a}kx}-\widehat{B}_0\right)\right)\Bigg|\end{aligned} \tag{59}$$

3. The series truncation error:

$$\begin{aligned}\epsilon_3 &:= \left|\int_a^b G(e^{z+x})f(z)\mathrm{d}z-e^{\zeta x}\left(2\sum_{k=0}^{N}\widehat{B}_k e^{i\frac{2\pi}{b-a}kx}-\widehat{B}_0\right)\right| \\ &= \left|2e^{\zeta x}\sum_{k=N+1}^{\infty}\widehat{B}_k e^{i\frac{2\pi}{b-a}kx}\right|\end{aligned} \tag{60}$$

If we introduce the concept of the cumulative probability density function (CDF) $F(z)$ such that $f(z)dz = dF(z)$, we can simplify the integration truncation error as follows:

$$
\begin{aligned}
\epsilon_1 &= \left| \left(\int_{-\infty}^{+\infty} G(e^{z+x}) f(z) \mathrm{d}z - \int_a^b G(e^{z+x}) f(z) \mathrm{d}z \right) \right| \\
&= \left| \left(\int_{-\infty}^{a} G(e^{z+x}) f(z) \mathrm{d}z + \int_b^{+\infty} G(e^{z+x}) f(z) \mathrm{d}z \right) \right|. \\
&\leq \left| \left(\int_{-\infty}^{a} \frac{\partial G(e^{z+x})}{\partial z} (F(z)) \mathrm{d}z \right) \right| + \left| \int_b^{+\infty} \frac{\partial G(e^{z+x})}{\partial z} (1 - F(z)) \mathrm{d}z \right| \qquad (61) \\
&\approx 0 : \quad (\text{if } z = a, b, -\infty, +\infty) \qquad (62)
\end{aligned}
$$

We can see that ϵ_1 is both bounded and approaches zero as long as $[a, b]$ is chosen reasonably such that $1 - F(b) \approx 0$ when $b < +\infty$ or $F(a) \approx 0$ when $a > -\infty$. We are also able to adapt the same idea to investigate the bound of ϵ_2. Accordingly, taking into account $|\exp(i\widetilde{\omega}_k z)| \leq 1$, we first investigate the error

$$
\underline{\epsilon}_2 := \left| \int_a^b f(y) e^{-i\widetilde{\omega}_k z} \mathrm{d}z - \phi\left(\widetilde{\omega}_k\right) \right|
$$

in ϵ_2. If we expand the equation above, we obtain

$$
\begin{aligned}
\underline{\epsilon}_2 &:= \left| \int_a^b f(z) e^{i\widetilde{\omega}_k z} \mathrm{d}z - \phi\left(\widetilde{\omega}_k\right) \right| \qquad (63) \\
&\leq \left| \left(\int_{-\infty}^{a} f(y) \mathrm{d}y + \int_b^{\infty} f(z) \mathrm{d}z \right) \right| \qquad (64) \\
&= |F(\infty) - F(b) + F(a) - F(-\infty)| \qquad (65) \\
&\approx 0 : \quad (\text{if } y = a, b, -\infty, \infty). \qquad (66)
\end{aligned}
$$

Based on the result above and the existence of the closed-form expression of $\widehat{G}(-\widetilde{\omega}_k) = \int_a^b G(e^y) e^{-i\widetilde{\omega}_k y} \mathrm{d}y$ in the Fourier space, we obtain

$$
\begin{aligned}
\epsilon_2 := \Bigg| & e^{\zeta x} \left(2 \sum_{k=0}^{N} \left(\frac{1}{b-a} \int_a^b G(e^y) e^{-i\widetilde{\omega}_k y} \mathrm{d}y \int_a^b f(z) e^{i\widetilde{\omega}_k z} \mathrm{d}z \right) e^{i\frac{2\pi}{b-a}kx} - \right. \\
& \left. \frac{1}{b-a} \int_a^b G(e^y) e^{-i\widetilde{\omega}_k y} \mathrm{d}y \int_a^b f(z) e^{i\widetilde{\omega}_0 z} \mathrm{d}z \right) - \left(e^{\zeta x} \left(2 \sum_{k=0}^{N} \widehat{B}_k e^{i\frac{2\pi}{b-a}kx} - \widehat{B}_0 \right) \right) \Bigg| \qquad (67) \\
= \Bigg| & e^{\zeta x} \left(2 \sum_{k=0}^{N} \frac{1}{b-a} \widehat{G}\left(-\widetilde{\omega}_k\right) \left(\int_a^b f(z) e^{i\widetilde{\omega}_k z} \mathrm{d}z - \phi(\widetilde{\omega}_k) \right) e^{i\frac{2\pi}{b-a}kx} - \right. \\
& \left. \frac{1}{b-a} \widehat{G}\left(-\widetilde{\omega}_0\right) \left(\int_a^b f(z) e^{i\widetilde{\omega}_0 z} \mathrm{d}z - \phi(\widetilde{\omega}_0) \right) \right) \Bigg| \qquad (68) \\
\leq \Bigg| & e^{\zeta x} \left(2 \sum_{k=0}^{N} \frac{1}{b-a} \widehat{G}\left(-\widetilde{\omega}_k\right) - \frac{1}{b-a} \widehat{G}\left(-\widetilde{\omega}_0\right) \right) \Bigg| \underline{\epsilon}_2. \qquad (69)
\end{aligned}
$$

Finally, the series truncation error is also bounded and can be formulated as follows:

$$\epsilon_3 = \left| 2e^{\zeta x} \sum_{k=N+1}^{\infty} \widehat{B}_k e^{i\frac{2\pi}{b-a}kx} \right| \leq 2e^{\zeta x} \sum_{k=N+1}^{\infty} \left| \widehat{B}_k \right|. \tag{70}$$

According to Theorem 4 (Luke, 1969, 271), Luke suggests that $|\sum_{k=N+1}^{\infty} b_k e^{i\frac{2\pi}{b-a}kz}|$ vanishes at least (N+1) times in $[a, b]$. Hence, ϵ_3 is bounded and approaches zero when N increases. Furthermore, according to Proposition 4.3 (Fang and Oosterlee, 2008, 11), since the complex Fourier series has geometrical convergence, we can see that

$$\epsilon_3 < P \exp(-(N-1)\nu),$$

where $\nu > 0$ is a constant and P is a term that varies less than exponentially with N.

Before we illustrate the total error bound when approximating any true European-type option price $V(x, t)$ defined as

$$\epsilon := \left| V(x,t) - e^{-r(T-t)-\zeta x} \mathfrak{Re} \left(2 \sum_{k=0}^{N} \widehat{B}_k e^{i\frac{2\pi}{b-a}kx} - \widehat{B}_0 \right) \right|, \tag{71}$$

we first summarise the whole approximation procedure of European-type option prices and note where ϵ_1, ϵ_2, and ϵ_3 lie. We start by seeking a definite interval $[a, b]$ that allows us to approximate $V(x, t)$ defined on $[-\infty, \infty]$ in (11) with the form

$$V(x,t) \approx e^{-r(T-t)} \int_a^b G(e^{x+z}, K) f(z) \mathrm{d}z,$$

in (12). The interval $[a, b]$ we propose satisfies condition (2). As a result, we obtain our first approximation error ϵ_1. As $V(x, t)$ is now approximated in $[a, b]$, this implies that we can construct a CFS expansion of $V(x, t)$, like the one in (56). Then, because including a characteristic function $\phi(\cdot)$ in the CFS expansion allows for a more accurate approximation, we have ϵ_2, an approximation error of $\frac{1}{b-a}\int_a^b G(e^y)e^{-i\widetilde{\omega}_k y}\mathrm{d}y \int_a^b f(z)e^{i\widetilde{\omega}_k z}dz$ in (22) with $\widehat{B}_k$ in (23). Finally, ϵ_3 is the series truncation error ϵ_3 in (56).

Finally, combining the results of ϵ_1, ϵ_2 and ϵ_3, we can first determine the total error bound ϵ of the European-type option; hence, we have an inequality of

$$\begin{aligned} \epsilon &= \left| e^{-r(T-t)} \left(\int_{-\infty}^{+\infty} G(e^{z+x}) f(z) \mathrm{d}z - e^{\zeta x} \mathfrak{Re} \left(2 \sum_{k=0}^{N} \widehat{B}_k e^{i\frac{2\pi}{b-a}kx} - \widehat{B}_0 \right) \right) \right| \\ &\leq |e^{-r(T-t)}| \left(\left| \int_{-\infty}^{+\infty} G(e^{z+x}) f(z) \mathrm{d}z - \int_a^b G(e^{z+x}) f(z) \mathrm{d}z \right| \right. \end{aligned}$$

$$
\begin{aligned}
&+ e^{\zeta x}\Bigg| 2\sum_{k=0}^{N}\frac{1}{b-a}\widehat{G}\left(-\frac{2\pi k}{(b-a)}-\zeta i\right)\left(\int_a^b f(z)e^{i\left(\frac{2\pi k}{(b-a)}+\zeta i\right)z}\mathrm{d}z\right)e^{i\frac{2\pi}{b-a}kx} \\
&\quad -\frac{1}{b-a}\widehat{G}\left(-\zeta i\right)\left(\int_a^b f(z)e^{i(\zeta i)z}\mathrm{d}z\right)-\left(2\sum_{k=0}^{N}\widehat{B}_k e^{i\frac{2\pi}{b-a}kx}-\widehat{B}_0\right)\Bigg| \\
&\quad\quad +\left|\sum_{k=N+1}^{\infty}2e^{\zeta x}\widehat{B}_k e^{i\frac{2\pi}{b-a}kx}\right|\Bigg) \\
&\leq |e^{-r(T-t)}|(\epsilon_1+\epsilon_2+\epsilon_3) \\
&< |e^{-r(T-t)}|(\epsilon_1+\epsilon_2+P\exp(-(N-1)\nu)) \qquad (72)
\end{aligned}
$$

Unfortunately, according to Fang and Oosterlee [cf. Proposition 4.2 and Lemma 4.3], the luxury of having an exponential convergence rate is lost if the rate becomes algebraic when we apply the complex Fourier expansion series around/at a discontinuity regarding one of its derivatives in a probability density function, such as VG's. In this case, a new bound can be constructed as follows:

$$
\epsilon_3 < \frac{\hat{P}}{(N-1)^{\beta-1}}. \qquad (73)
$$

Here, $\hat{P}$ is a constant and $\beta \geq n \geq 1$ (n is the algebraic index of convergence of $e^{i\frac{2\pi}{b-a}kz}$). Using the aforementioned error bound, we can see that the total error bound ϵ is bounded by

$$
|e^{-r(T-t)}|\left(\epsilon_1+\epsilon_2+\frac{\hat{P}}{(N-1)^{\beta-1}}\right) \qquad (74)
$$

A chooser option is a combination of a call and a put with different time-to-maturity for each option. Hence, as the Fourier transforms of both payoff functions exist in the chooser option, we can directly apply (72) and (74) to conclude that the total error bound of a chooser option is bounded and tends to zero when the number of the $e^{i\frac{2\pi}{b-a}kz}$ terms increases. Finally, the total error of any option on a forward (futures) contract is also bounded by (72) and (74) because the CFS pricing formulae (38) and (41) are exactly the same as that of (14) but with input values of $\hat{x}$ and $\overline{x}$, respectively.

6. Numerical Results

In this section, we demonstrate the performance of the CFS method through a number of numerical experiments. The purpose of this section is to test whether the error convergence analysis presented in section 5 is in line with the numerical findings in this section. Moreover, we also test the theoretical capability of the CFS method to price any deep in(out)-of-the-money European-type options under different models.

As the CGMY model with the condition that the parameter Y is close to 2 represents a distribution with very heavy tails (cf. Appendix A), it is worth testing whether it is feasible or possible for this method to address this extreme condition. Throughout the experiments, we choose long and short maturities to test the CFS method. We compare our results generated by the CFS method with those of the COS method (Fang and Oosterlee, 2008) and the CONV method (an FFT method, Lord et al. 2008). When we implement the CONV method, we use Simpson's rule for the Fourier integrals to achieve fourth-order accuracy. From these numerical experiments and comparisons with other methods, we confidently demonstrate the stability and robustness of the CFS method for both normal and extreme conditions. In all numerical experiments, by trial and error, if we set $\zeta = 0.5$ in the multiplication factor $\exp(\zeta x)$, we can guarantee the existence of $\widehat{G}(\cdot)$ and $\widehat{G}_1(\cdot)$. Furthermore, to avoid confusion, in the experiments, we use parameter N and denote the number of terms of the CFS method and the COS method and the number of grid points for the CONV method. All CPU times presented (in milliseconds) are determined after averaging the computational times of 150 experiments. A MacBook Pro is used for all experiments with a 2.8 GHz Intel Core i7 CPU and two 8GB DDR SDRAMs (cache memory). The code is written in MATLAB R2011b.

In all tables, we examine only the time-to-maturity T of the European options in the range from 0.1 to 10. The parameter L in the truncated interval $[a, b]$ is also chosen in the range of 10 to 12. In general, allowing for larger values of L yields a larger range of truncated intervals and leads to larger values of N to reach the same level of accuracy. Each table presents comparisons of the methods in terms of CPU time usage and the maximum absolute error in ascending order of N. In all tables, we can see that there is little difference between the CFS method and the COS method in terms of CPU time usage; however, the CONV method unquestionably consumes more CPU time than the other two to yield a desirable result in each experiment.

To investigate the error convergence, in the first six tables of the numerical experiments, we test and compare the CFS method with the COS method and the CONV method for vanilla calls using the BS model (Table 2), vanilla puts with the Meixner model (Table 3), a cash-or-nothing call using the BS model (Table 4), a cash-or-nothing put using the FMLS model (Table 5), an asymmetric put using the NIG model (Table 6), a symmetric put using the BS model (Table 7) and a chooser option using the BS model (Table 8). Overall, from the numerical experiments, we can see that the CFS method outperforms both the COS method and the CONV method because the CFS method yields an extremely small maximum absolute error with a small value of N. In addition, the exponential convergence rate obtained in the experiments is consistent with the theoretical findings in section 5. In Table 3, we vary the strike prices among three values (80, 100 and 120) to test the feasibility of the methods. Surprisingly, the COS method cannot yield a convergence rate with the large maximum error expected with the strike price at 80 in Table 3. This result contradicts the error analysis suggested in Fang and Oosterlee (2008). The results in Table 2 and Table 3 suggest that the CONV method requires substantial amounts of CPU time and large N

Table 2: Error convergence and CPU time comparing the CFS method with the COS and CONV methods for European calls using the BS model, parameters as in Fig. 1; $K = 80,\ 100,$ and 120; reference val.= 20.799226309..., 3.659968453..., and 0.044577814..., respectively.

	N	8	16	32	64	128
CFS	msec.	0.099	0.123	0.211	0.412	0.734
	max abs. error	1.623E-01	2.776E-04	5.684E-14	1.984E-14	1.984E-14
COS	msec.	0.102	0.193	0.231	0.442	0.754
	max abs. error	4.427E-01	5.913E-03	9.139E-08	1.887E-14	1.887E-14
CONV	msec.	0.112	0.189	0.211	0.432	0.774
	max abs. error	76.297	64.561	22.754	1.040	0.2659

Table 3: Error convergence and CPU time comparing the CFS method with the COS and CONV methods for European puts using the Meixner model, parameters as in Fig. 2; $K = 80,\ 100,$ and 120; reference val.= $7.811229572E{-}14$, 0.00861873646..., and 16.453464059..., respectively.

	N	16	32	64	128	256	512
CFS	msec.	0.123	0.211	0.412	0.734	1.071	1.932
	max abs. error	0.1556	1.642E-04	1.380E-03	7.740E-07	1.249E-16	1.249E-16
COS	msec.	0.124	0.221	0.442	0.824	1.121	2.032
	max abs. error	1.788E-02	2.864E-02	2.864E-02	2.864E-02	2.864E-02	2.864E-02
CONV	msec.	0.211	0.432	0.774	0.921	1.189	2.345
	max abs. error	4.7689	1.856	1.044	0.741	0.264	2.825E-02

to reach a fourth-order convergence rate. All results in the two tables are illustrated graphically in Figures 1 and 2. It is also notable that the reference value suggested by Fang and Oosterlee (2008) is not correct when we price a cash-or-nothing call using the BS model. As we benchmark the value using a standard (a MATLAB Financial Toolbox function called cashbybls), it should be 0.00277554137..., as shown in Table 4. The second row of the table related to the CPU time and the maximum absolute error of the COS method is copied from Fang and Oosterlee (2008). The COS method does not appear to be a good choice for evaluating the option because it requires $N = 80$ to reach a maximum absolute error of $6.35E-04$; however, only $N = 32$ is required to yield a maximum absolute error of $1.462E-16$ in the CFS method.

The CFS method is comparable to the COS method when it addresses pricing far deep (in)-out-of-the-money options. Tables 9 (a far deep in-the-money option using the BS model) and 10 (a far deep out-of-the-money option using the Merton model) show that the CONV method is incapable

Table 4: Error convergence and CPU time comparing the CFS method with the COS method for European cash-or-nothing calls using the BS model with S=100, $K = 120$, $r = 0.05$, $q = 0$, $T = 0.1$, and $\sigma = 0.2$; reference val.= 0.00277554137.... The parameters are taken from Fang and Oosterlee (2008).

	N	8	16	32	64	128
CFS	msec.	0.313	0.343	0.391	0.430	0.523
	max abs. error	2.012E-03	1.161E-05	1.461E-16	1.461E-16	3.599E-17
	N	40	60	80	100	120
COS	msec.	0.330	0.334	0.376	0.428	0.486
	max abs. error	2.46E-02	1.64E-02	6.35E-04	6.85E-06	2.44E-08

Table 5: Error convergence and CPU time of the CFS method for a European cash-or-nothing put using the FMLS model with $S = 100$, $K = 120$, $r = 0.03$, $q = 0.01$, $T = 10$, $\sigma = 0.1486$, $\alpha = 1.5597$, and $L = 10$; reference val.= 15.035244109 . . . . The parameters are taken from Fang and Oosterlee (2008).

	N	8	16	32	64	128
CFS	msec.	0.314	0.329	0.401	0.450	0.601
	max abs. error	2.025E-04	1.341E-08	1.361E-16	1.361E-16	1.36E-16

Table 6: Error convergence and CPU time of the CFS method for a European asymmetric put option with a payoff of $(S_T^3 - K^3)$ put using the NIG model; $S = 90$, $K = 100$, $r = 0.03$, $q = 0$, $T = 0.5$, $\alpha = 6.1882$, $\beta = -3.8941$, $\delta = 0.1622$, and $L = 10$; reference val.= 203704.644879212 . . . .

	N	8	16	32	64	128
CFS	msec.	0.245	0.399	0.614	0.8423	1.801
	max abs. error	6.025E-1	1.213E-05	1.343E-14	1.343E-14	1.343E-14

Table 7: Error convergence and CPU time of the CFS method for a European symmetric call option with a payoff of $(S_T - K)^2$ put using the BS model; $S = 120$, $K = 100$, $r = 0.02$, $q = 0.2$, $T = 1$, $\sigma = 0.25$, and $L = 10$; reference val. = 384.974699787 . . . .

	N	8	16	32	64	128
CFS	msec.	0.413	0.589	0.714	0.9233	2.100
	max abs. error	-28.5925	1.665E-03	1.819E-12	1.819E-12	1.819E-12

Table 8: Error convergence and CPU time of the CFS method for a European Chooser option using the BS model; $S = 5$, $K = 1$, $r = 0.1$, $q = 0.01$, $T_c = 0.5T = 1$, $\sigma = 0.2$, and $L = 10$; reference val.= 4.024540221 . . . .

	N	8	16	32	64	128
CFS	msec.	0.240	0.391	0.623	0.8523	1.901
	max abs. error	2.173E-02	1.834E-02	3.660E-04	2.226E-11	0

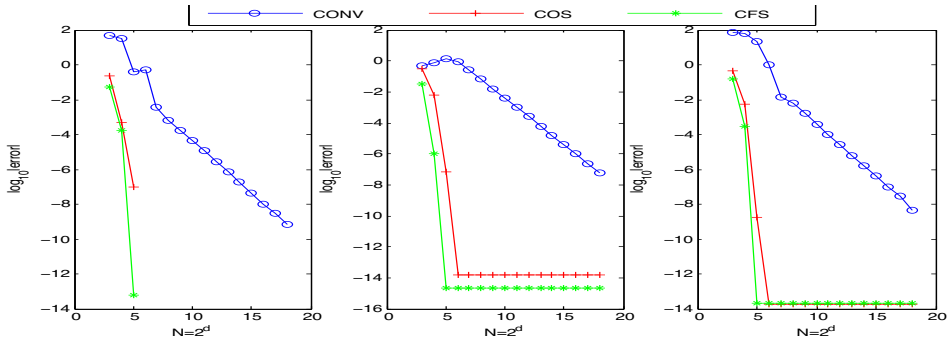

Figure 1: CFS vs. CONV and COS in error convergence for pricing European call options using the GBM model with $S = 100$, $r = 0.1$, $q = 0$, $T = 0.1$, $\sigma = 0.25$, $L = 10$ and $K = 80$ (left figure), $= 100$ (middle figure) and $= 120$ (right figure). The parameters are taken from Fang and Oosterlee (2008).

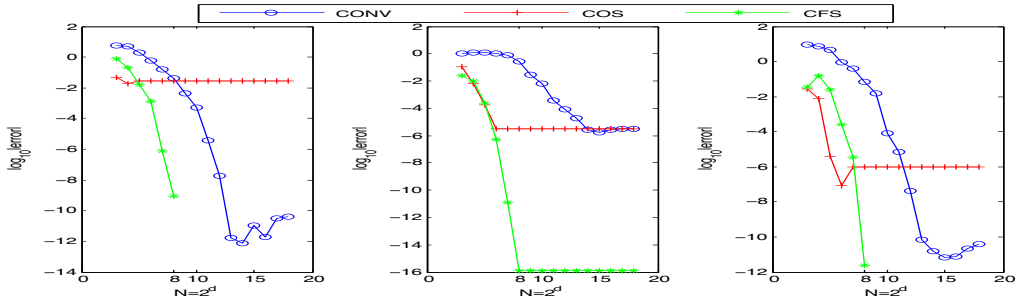

Figure 2: CFS vs. CONV and COS in error convergence for pricing European put options using the Meixner model with $S = 100$, $r = 0.06$, $q = 0$, $T = 0.5$, $\alpha = 0.02982825$, $\delta = 0.57295483$, $\beta = 0.12716244$, $L = 12$, and $K = 80$ (left figure), $= 100$ (middle figure) and $= 120$ (right figure). Parameters are taken from Schoutens (2002).

Table 9: Error convergence and CPU time comparing the CFS method with the COS and CONV methods for a European deep in-the-money call using the BS model with $S = 100$ and $K = 50$; reference val. $= 50.49750831254\ldots$. The parameters are taken from Figure 1.

	N	32	64	128	256	512	1028
CFS	msec.	0.231	0.431	0.714	1.081	2.111	2.965
	max abs. error	0.343	0.309	9.323E-03	6.250E-07	5.911E-14	2.311E-14
COS	msec.	0.235	0.441	0.754	1.186	2.211	3.265
	max abs. error	0.143	0.509	7.323E-03	6.45E-07	5.922E-13	2.451E-13
CONV	msec.	0.211	0.412	0.734	1.189	2.311	3.245
	max abs. error	99.995	99.995	99.995	99.995	99.995	99.995

of pricing the option and that both the CFS and COS methods are very accurate and yield an exponential convergence rate. The nature of the moneyness levels we consider here is quite extreme and, practically, is not common in financial markets. The purpose of having Tables 9 and 10 is to show the robustness of the CFS method theoretically.

In Tables 11 and 12, it is clear that the maximum absolute errors of both the CFS method and the COS method are similar for European calls using the VG model. We have an exponential convergence rate when $T = 1$ but an algebraic convergence rate when $T = 0.1$ because, as illustrated in Figure 3, the recovered VG density function has an abrupt point at the origin when $T = 0.1$. In terms of testing the methods for European calls using the Heston model, an affine stochastic volatility model, the CFS method converges more quickly than the COS method to reach a desirably

Table 10: Error convergence and CPU time comparing the CFS method with the COS and CONV methods for a European deep out-of-the-money put using the Merton model with $S = 100$, $K = 50$, $r = 0.05$, $q = 0.2$, $T = 0.25$, $\sigma = 0.15$, $\lambda = 0.1$, $\mu_J = 0$, $\sigma_J = 0.45$ and $L = 10$; reference val. $= 0.0166841187\ldots$.

	N	32	64	128	256	512	1028
CFS	msec.	0.241	0.441	0.764	1.121	2.011	3.015
	max abs. error	0.251	0.0423	5.061E-04	5.643E-11	1.211E-13	1.211E-14
COS	msec.	0.231	0.431	0.674	1.361	2.411	3.215
	max abs. error	0.355	0.06575	7.011E-04	7.733E-11	2.311E-14	5.455E-14
CONV	msec.	0.257	0.456	0.687	1.121	2.245	3.347
	max abs. error	5.276E-03	5.335E-03	5.337E-03	5.337E-03	5.337E-03	5.337E-03

Table 11: Error convergence and CPU time comparing the CFS method with the COS method for a European call using the VG model with $S = 100$, $K = 90$, $r = 0.1$, $T = 1$, $q = 0$, $\sigma = 0.12$, $\theta = -0.14$, and $\nu = 0.2$; reference val. $= 19.099354724\ldots$. The parameters are as in Fang and Oosterlee (2008).

	N	32	64	96	128	160
CFS	msec.	0.223	0.429	0.634	0.8023	1.674
	max abs. error	1.043E-04	4.32E-07	5.040E-09	1.483E-10	1.114E-11
COS	msec.	0.235	0.441	0.654	0.7923	1.534
	max abs. error	5.099E-04	1.308E-06	2.129E-08	1.723E-09	5.542E-11

Table 12: Error convergence and CPU time comparing the CFS method with the COS method for a European call using the VG model. The parameters are as in Table 11 but with $T = 0.1$; reference val. $10.993630572\ldots$.

	N	32	64	128	256	512	1024
CFS	msec.	0.223	0.439	0.794	1.231	1.974	2.131
	max abs. error	4.086E-03	4.227E-03	5.576E-04	2.315E-04	1.237E-4	7.941E-05
COS	msec.	0.223	0.450	0.894	1.234	2.074	2.431
	max abs. error	1.530E-03	5.010E-04	1.170E-05	7.171E-05	7.260E-05	7.256E-05

small maximum absolute error, as shown in Tables 13 and 14. Moreover, as shown in Figure 4, we obtain algebraic convergence for the CFS method due to the appearance of a non-smooth point at the origin when $T = 1$.

As there are no reference values available for the CGMY model, the reference values for these models are computed using the CFS method, with $N = 2^{22}$. In the numerical experiments for the CGMY model (cf. Tables 15, 16 and 17), although the reference values are generated using the CFS method, the differences between them and those generated using the COS method are approximately $1E - 14$. As shown in Figure 5, the error convergence of the CFS method under the CGMY model is exponential and superior to that of the CONV method and the COS Method. In Table 17, when the value of Y is equal to 1.98 (implying that the model is heavily fat-tailed), the CFS method remains able to very effectively cope with this extreme condition. To the best of our knowledge, apart from the COS method, no numerical method can accurately price options for very large $Y \approx 2$ in a robust manner.

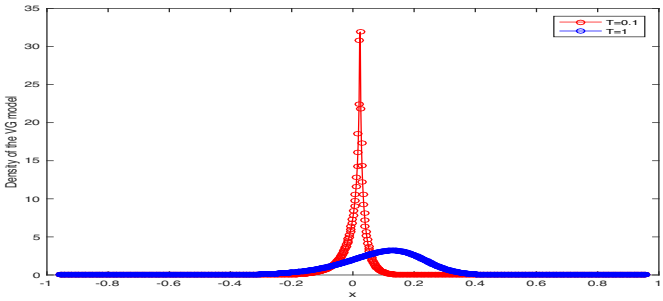

Figure 3: Recovered Densities of the VG experiments; the parameters are as in Table 11 and Table 12.

Table 13: Error convergence and CPU time comparing the CFS method with the COS and CONV methods for a European call using the Heston model with $S = 100$, $K = 100$, $r = 0$, $T = 1$ $q = 0$, $u_0 = 0.0175$, $\overline{u} = 0.0398$, $\lambda = 1.5768$, $\eta = 0.5751$, $\rho = 0.5711$ and $L = 12$; reference val. $= 5.785155450\ldots$. The parameters are as in Fang and Oosterlee (2008).

	N	64	128	256	512	1024	2048
CFS	msec.	0.429	0.634	0.8023	1.674	2.145	4.125
	max abs. error	0.1803	1.399E-02	8.740E-05	1.599E-08	1.599E-08	1.599E-08
COS	msec.	0.429	0.624	0.7023	1.604	2.235	4.525
	max abs. error	0.6380	2.685E-02	3.343E-03	1.370E-05	1.508E-08	1.562E-08
CONV	msec.	0.456	0.777	1.341	2.565	3.567	6.786
	max abs. error	7.381E-02	0.2834	5.563E-02	1.399E-02	3.497E-03	8.741E-04

Table 14: Error convergence and CPU time comparing the CFS method with the COS and CONV methods for a European call using the Heston model. The parameters are as in Table 13 but with $T = 10$; reference val. $= 22.318945791\ldots$.

	N	64	128	256	512	1024	2048
CFS	msec.	0.428	0.635	0.8103	1.644	2.245	4.105
	max abs. error	4.994E-02	6.280E-04	7.603E-09	1.544E-10	1.544E-10	1.544E-10
COS	msec.	0.430	0.624	0.902	1.614	2.235	4.595
	max abs. error	1.069	1.018E-02	4.890E-05	3.81231E-10	1.545E-10	1.545E-10
CONV	msec.	0.456	0.801	1.345	2.865	3.667	6.986
	max abs. error	0.3954	0.6231	0.7225	0.7691	0.7917	0.8028

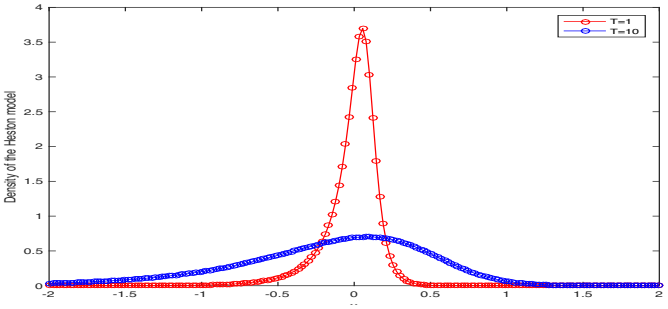

Figure 4: Recovered density functions of the Heston experiments; the parameters are taken from Table 13 and Table 14.

Table 15: Error convergence and CPU time comparing the CFS method with the COS and CONV methods for a European call option using the CGMY model. The parameters are as in Figure 5 but with $Y = 0.5$; reference val. $= 19.812948842\ldots$.

	N	16	32	64	128	256	512
CFS	msec.	0.221	0.434	0.744	1.171	1.320	1.601
	max abs. error	0.168	1.485E-03	6.564E-07	3.155E-12	0	0
COS	msec.	0.230	0.452	0.834	1.201	1.523	1.834
	max abs. error	0.528	1.240E-02	2.800E-05	3.595E-09	1.207E-10	1.207E-10
CONV	msec.	0.344	0.528	0.917	1.316	1.623	1.931
	max abs. error	1.078	0.817	2.089E-01	5.176E-02	1.291E-02	3.226E-03

Table 16: Error convergence and CPU time in a comparison of the CFS method with the COS and CONV methods for a European call option using the CGMY model. The parameters are as in Figure 5 but with $Y = 1.5$; reference val. $= 49.790905468\ldots$.

	N	8	16	32	64	128
CFS	msec.	0.124	0.221	0.434	0.744	1.171
	max abs. error	1.538	9.68E-04	2.700E-13	0	0
COS	msec.	0.130	0.230	0.452	0.834	1.201
	max abs. error	0.9303	2.86E-02	1.240E-05	3.410E-13	3.410E-13
CONV	msec.	0.329	0.344	0.528	0.917	1.316
	max abs. error	5.245	0.776	0.760	1.756	2.434

Table 17: Error convergence and CPU time comparing the CFS method with the COS and CONV methods for a European option using the CGMY model. The parameters are as in Figure 5 but with $Y = 1.98$; reference val. $= 99.999905509\ldots$.

	N	8	16	32	64	128
CFS	msec.	0.124	0.221	0.434	0.744	1.171
	max abs. error	5.866E-01	7.640E-05	0	0	0
COS	msec.	0.130	0.230	0.452	0.834	1.201
	max abs. error	1.532	2.551E-02	1.7870E-06	3.81231E-10	6.843E-10
CONV	msec.	0.329	0.344	0.528	0.917	1.316
	max abs. error	289.45	593.12	838.93	998.08	798.08

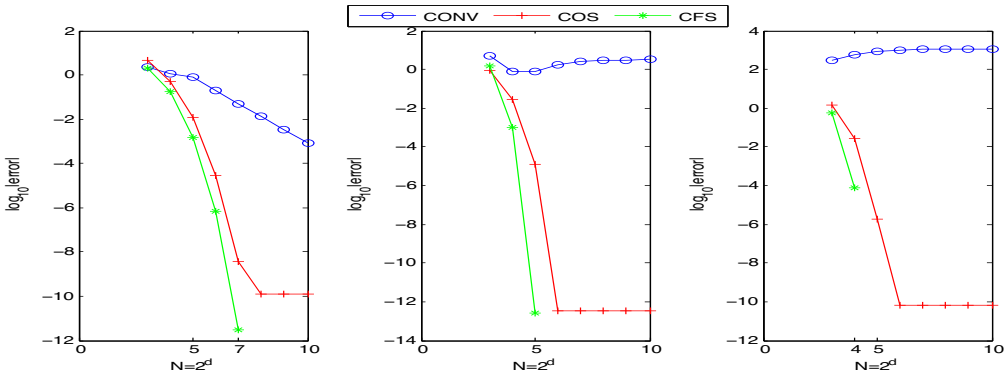

Figure 5: CFS vs. CONV and COS in error convergence for pricing European call options using the CGMY model with $S = 100$, $K = 100$, $r = 0.1$, $T = 1$ $q = 0$, $C = 1$, $G = 5$, $M = 5$, $Y = 0.5$, $L = 12$ and $Y = 0.5$ (left figure), $= 1.5$ (middle figure) and $= 1.98$ (right figure). The parameters are taken from Fang and Oosterlee (2008).

7. Conclusion and Discussion

In this paper, we introduced the CFS method to derive European-style option pricing formulas. This method can be used when both the characteristic function of the underlying price process and its payoff functions are analytically traceable. The CFS method is based on the notion of representing option prices with a truncated series sum of complex exponential functions and their respective coefficients. The CFS method yields numerical computations of the pricing formulas that are easy to implement and highly efficient.

We performed an error analysis in addition to deriving the CFS method. In the error analysis, we first showed that choosing a suitably large interval $[a, b]$ plays a crucial role in reducing the integration truncation error (58) and the error related to approximating $\frac{1}{b-a}\int_a^b G(e^y)e^{-i\widetilde{\omega}_k y}\mathrm{d}y\int_a^b f(z)e^{i\widetilde{\omega}_k z}dz$ with $\widehat{B}$ (59). Moreover, combined with the analysis of the truncated summation error (60), we gained an exponential convergence rate for a smooth PDF. This theoretical finding is in accordance with the numerical experimental results. However, when the PDF of the underlying process has a discontinuity in one of its derivatives, algebraic convergence was expected and proven as such in the error analysis; this result was also observed in the numerical experiments. Our error analysis differs from that of Fang and Oosterlee (2008), as we clearly show that all truncation errors–(58), (59) and (60) are equally pivotal in determining the convergence rate of the CFS method.

In the numerical experiments, in terms of the accuracy of pricing in(out)-of-the-money options, the performance of the CFS method was occasionally the same as and frequently better than that of the COS method (e.g., Table 4). Additionally, in some numerical results, the COS method was unable to yield a convergence rate as the number of the cosine terms N increased. This result contradicts the error analysis of Fang and Oosterlee (2008). Finally, very rapid computing times are reported here for Lévy models and affine stochastic volatility both with and without jumps. For $N < 150$, all numerical results (except for the VG model with $T = 0.1$) were accurate up to 9 digits and obtained in less than 0.5 milliseconds of CPU time.

Although the theoretical analysis/numerical results presented here have demonstrated the effectiveness of the CFS method, it might be further developed in three ways. First, whether the CFS method can be applied to price European-type basket options is an interesting research question. A basket option is a financial derivative, and the risk of its underlying asset is a weighted sum of the different assets that have been grouped together in the basket. Based on the properties of basket options, pricing such options entails the well-known higher-dimensional problem and is therefore subject to the curse of dimensionality. One possible method for solving this problem is to apply parallel partitioning (Leentvaar and Oosterlee, 2008), a computational algorithm that allows for rapid computation of higher-dimensional problems, to the CFS method. Second, we note that some underlying process PDFs, with a short time to maturity, such as that of VG, can ruin the exponential convergence rate of the CFS method when it is used to recover the PDF because the PDF has a discontinuity in one of its derivatives. In future work, to avoid this problem, we can

apply filters (Vandeven, 1991; Tadmor and Tanner, 2005) to the CFS method; this strategy is a numerical method for modifying the Fourier coefficients to maintain an exponential convergence rate of Fourier series expansions. Finally, the accuracy of the CFS pricing formulae depends on the choice of ζ of the damping factor $\exp(\zeta x)$, and ζ is chosen by trial and error in this paper. As we see it as the future development of the CFS method, we will look into finding the optimal value of ζ theoretically.

Appendix A. Stochastic Processes in Financial Markets

In this section, we briefly review four popular stochastic processes—the exponential Lévy process and affine stochastic volatility model. The example processes we demonstrate in this section are either relatively commonly applied in financial markets or are difficult to implement for option pricing via other numerical methods. Our CFS approximation method is not limited to the examples we present in this section but can be used for any process when its characteristic function exists. A standard reference for these processes is Schoutens (2003) or Cont and Tankov (2004). Throughout this section, to ensure that each process is a martingale process, we also define a risk-fee drift of $\gamma_c t$ as $(r-q)t+\omega$ and ω, a drift-compensation term, which is equal to $\log\phi(-i)-(r-q)t$.

Appendix A.1. Exponential Lévy Processes

Appendix A.1.1. The Brownian process

Suppose that we have the BSM model (a geometric Brownian process) Black and Scholes (1973) and Merton (1973) L_t^{BS} with a drift $\gamma_c = r - q - \frac{1}{2}\sigma^2$ given by

$$L_t^{\mathrm{BSM}} = \gamma_c t + \sigma W_t, \tag{A.1}$$

where W_t is a risk-neutral Brownian motion with $W_0 = 0$ and σ is the volatility. Then, the characteristic function of this process is

$$\begin{aligned} \mathbb{E}[e^{izL_t^{(\mathrm{BSM})}}] &:= \phi(z) \\ &= \exp\left(t\left(iz\gamma_c - \frac{1}{2}\sigma^2 z^2\right)\right),\ z\in\mathbb{R}. \end{aligned} \tag{A.2}$$

Appendix A.1.2. The Lévy Jump-diffusion Model

A Lévy jump diffusion process is a Lévy process in which the jump component is given as a compound Poisson process. It can be represented in the following form:

$$L_t^{(\mathrm{JD})} := \gamma_c t + \sigma W_t + \sum_{i=1}^{N_t} Y_i, \tag{A.3}$$

where $\gamma_c \in \mathbb{R}$ is a drift term; $\sigma > 0$, $(W_t)_{t\geq 0}$ denotes Brownian motion; $(N_t)_{t\geq 0}$ is an independent Poisson process with intensity λ; and $(Y_i)_{i\geq 1}$ is an independent, identically distributed (i.i.d.) sequence of random variables that are independent of both $(N_t)_{t\geq 0}$ and $(W_t)_{t\geq 0}$.

Appendix A.1.3. The Merton Model

The classical Merton jump-diffusion model with Gaussian jumps (Merton, 1976) was introduced to include jumps in the modelling of log-prices X_t. In this model, Y_i are normally distributed $\mathbb{N}(\mu_J, \sigma_J^2)$. Thus, this is a Lévy process with the following characteristic function:

$$\begin{aligned}\mathbb{E}\left[e^{izL_t^{(\mathrm{MJ})}}\right] &:= \phi(z) \\ &= \exp\left(t\left(iz\gamma_c - \frac{\sigma^2 z^2}{2} + \lambda\big(e^{-\sigma_J^2 z^2/2 + iz\mu_J} - 1\big)\right)\right),\ z \in \mathbb{R}. \end{aligned} \tag{A.4}$$

Appendix A.1.4. The Kou Model

Another jump-diffusion-type Lévy model is the Kou model (Kou, 2002), which uses double-exponentially distributed jump size variables Y_i. The characteristic function of this process is

$$\begin{aligned}\mathbb{E}\left[e^{izL_t^{(\mathrm{Kou})}}\right] &:= \phi(z) \\ &= \exp\left(t\left(iz\gamma_c - \frac{\sigma^2 z^2}{2} + \lambda\big(\frac{p\alpha_1}{\alpha_1 - iz} + \frac{(1-p)\alpha_2}{\alpha_2 + iz} - 1\big)\right)\right),\ z \in \mathbb{R}, \end{aligned} \tag{A.5}$$

where $p \in [0,1]$ represents the probability of a jump and α_1 and α_2 control the decay of the tails of the distribution of positive and negative jump sizes, respectively. The two processes represent finite activity because $\nu(\mathbb{R}) < \infty$, but they represent infinite variation if $\sigma > 0$.

Appendix A.1.5. The Normal Inverse Gaussian Model

The normal inverse Gaussian (NIG) distribution is characterised by a normal inverse Gaussian mixing distribution. The characteristic function of NIG is given by

$$\begin{aligned}\mathbb{E}\left[e^{izL_t^{(\mathrm{NIG})}}\right] &:= \phi(z) \\ &= \exp\left(t\left(iz\gamma_c - \frac{1}{2}\sigma^2 z^2 + \delta\left(\sqrt{\alpha^2 - \beta^2} - \sqrt{\alpha^2 - (\beta + iz)^2}\right)\right)\right),\ z \in \mathbb{R}. \end{aligned} \tag{A.6}$$

Appendix A.1.6. The Meixner Model

The Meixner Model was studied and introduced by Schoutens and Teugels (1998) and Grigelionis (1999). The application of this model to finance was properly developed in Schoutens (2002). The density of the Meixner density distribution function is defined as

$$f_{\mathrm{Mex}}(z; \alpha, \beta, d) = \frac{(2\cos(\beta/2))^{2d}}{2\alpha\pi\Gamma(2d)} \exp\left(\frac{\beta z}{\alpha}\right) \left|\Gamma\left(d + i\frac{z}{\alpha}\right)\right|^2,$$

where $\alpha > 0$, $-\pi < \beta < \pi$, $d > 0$. The characteristic function of the Meixner model is given by

$$\mathbb{E}\left[e^{izL_t^{(\mathrm{Mex})}}\right] := \phi(z) \tag{A.7}$$

$$= \exp\left(iz\gamma_c t\right)\left(\frac{\cos(\beta/2)}{\cosh((\alpha z - i\beta)/2))}\right)^{2dt}, \; z \in \mathbb{R}. \tag{A.8}$$

Appendix A.1.7. The Variance Gamma Model

The variance gamma or the VG process (Madan and Seneta, 1990; Madan and Milne, 1991; Madan et al., 1998) is a subordinate version of Brownian motion (cf. Cont and Tankov, 2004). The most important feature of this model is that the Brownian motion is evaluated in *random time* t^* (determined by an independent increasing Lévy process—a gamma process) rather than in calendar time, t. Suppose that the VG process $b(t^*; \theta, \sigma)$ is defined as $\theta t^* + \sigma W_{t^*}$, where the random time t^* is given by a gamma process $\mathrm{Gamma(t}; 1, \upsilon)$ with a unit mean and variance υ, θ is a drift at t^*, and W_{t^*} denotes standard Brownian motion. Then, we define the VG process with a drift term γ_c as follows:

$$L_t^{(\mathrm{VG})} = \gamma_c t + \theta \mathrm{Gamma(t}; 1, \upsilon) + \sigma W_{\mathrm{Gamma(t};1,\upsilon)}, \tag{A.9}$$

where ω is the compensation term. A characteristic function for the variance gamma process is

$$\mathbb{E}\left[e^{izL_t^{(\mathrm{VG})}}\right] := \phi(z) \tag{A.10}$$

$$= \exp\left(iz\gamma_c t\right)\left(\frac{1}{1 - i\theta\upsilon z + \frac{\sigma^2\upsilon}{2}z^2}\right)^{\frac{t}{\upsilon}}, \; z \in \mathbb{R}. \tag{A.11}$$

The Lévy density function of the VG process can also be defined as

$$\nu_{(\mathrm{VG})}(dx) = \begin{cases} \frac{\mu_-^2}{\upsilon_-}\frac{\exp(-\mu_-/\upsilon_-|x|)}{|x|}dx, \; x < 0, \\ \frac{\mu_+^2}{\upsilon_+}\frac{\exp(-\mu_+/\upsilon_+|x|)}{|x|}dx, \; x \geq 0, \end{cases} \tag{A.12}$$

or

$$\nu_{(\mathrm{VG})}(dx) = \begin{cases} C\exp(-G|x|)/|x|dx, \; x < 0, \\ C\exp(-M|x|)/|x|dx, \; x \geq 0. \end{cases} \tag{A.13}$$

$C = 1/\upsilon > 0$, $M = 1/\vartheta_+ > 0$, $G = 1/\vartheta_- > 0$, $\vartheta_+ - \vartheta_- = \theta\upsilon$ and $\vartheta_+\vartheta_- = \sigma^2\upsilon/2$. From the Lévy measure, the VG process has infinite activity and finite variation (cf. Cont and Tankov, 2004). As it is an infinite activity jump process, the VG process is versatile enough to include both small jumps (to mimic a Brownian component) and large jumps. Consequently, unlike the jump-diffusion model, a Brownian component is no longer necessary in the VG process.

Appendix A.1.8. The CGMY Model

Carr et al. (2002) introduced a class of infinitely divisible distributions (also known as a tempered stable process Cont and Tankov 2004), which is an extended version of the VG process, in 2002. The Lévy measure for the CGMY process is given by

$$\nu_{(\mathrm{CGMY})}(dx) = \begin{cases} C\exp(-G|x|)/|x|^{Y+1}dx, \ x<0, \\ C\exp(-M|x|)/|x|^{Y+1}dx, \ x>0. \end{cases} \tag{A.14}$$

$C>0$, $G>0$, $M>0$, and $Y<2$. The parameter Y captures the fine structure of the process. For $Y<-1$, we obtain a compound Poisson process that has finite variation and finite activity. However, when $Y\in[0,1)$, the process has infinite activity and finite variation, which is similar to the VG process (we can see that when $Y=0$, this process is equivalent to the VG process). For $Y\in[1,2)$, the process has infinite activity and infinite variation. Based on the different values of Y, there are three different types of characteristic functions in the CGMY process. We summarise these in the following list:

$$\mathbb{E}\left[e^{izL_t^{(\mathrm{CGMY})}}\right] := \phi(z) \tag{A.15}$$

$$= \exp\left(t(iz\gamma_c + \int_{-\infty}^{\infty}(e^{izx}-1-izx)\nu(dx))\right) \ z\in\mathbb{R}. \tag{A.16}$$

- If $Y=0$,

$$\phi(z) = \exp\left(iz\gamma_c - C\left(\left(\frac{iz}{G}+\log\left(1+\frac{iz}{G}\right)\right)+\left(-\frac{iz}{M}+\log\left(1-\frac{iz}{M}\right)\right)\right)\right), \tag{A.17}$$

- if $Y=1$,

$$\phi(z) = \exp\left(iz\gamma_c + C\left((G+iz)\log\left(1+\frac{iz}{G}\right)+(M-iz)\log\left(1-\frac{iz}{M}\right)\right)\right), \tag{A.18}$$

- and if $Y\in(0,2)/\{1\}$,

$$\phi(z) = \exp\left(iz\gamma_c + C\Gamma(-Y)G^Y\left(\left(1+\frac{iz}{G}\right)^Y - 1 - \frac{izY}{G}\right)\right.$$
$$\left. + C\Gamma(-Y)M^Y\left(\left(1-\frac{iz}{M}\right)^Y - 1 + \frac{izY}{M}\right)\right). \tag{A.19}$$

We can also extend the CGMY model by adding a diffusion component, resulting in the following new form:

$$L_t^{\mathrm{CGMY_e}} = L_t^{\mathrm{CGMY}} + \sigma W_t,\ \sigma > 0, \tag{A.20}$$

with a characteristic function given by

$$\mathbb{E}\left[e^{izL_t^{(\mathrm{CGMY_e})}}\right] := \exp\left(t\frac{\sigma^2 z^2}{2}\right)\phi(z). \tag{A.21}$$

Appendix A.1.9. Finite Moment Log Stable

The Finite Moment Log Stable (FMLS) process is a Lévy process with infinite activity that was proposed by Carr and Wu (2003) to model S&P 500 index options where the volatility skew does not flatten as the time to maturity increases. The characteristic function of FMLS is described by

$$\begin{aligned}\mathbb{E}[e^{izL_t^{(\mathrm{FMLS})}}] &:= \phi(z) \\ &= \exp\left(t\left(iz\gamma_c - (iz\sigma)^\alpha \sec\left(\frac{\pi\alpha}{2}\right)\right)\right).\end{aligned} \tag{A.22}$$

The tail index $\alpha \in (1, 2]$ is designed to control the tail behaviour of a PDF, and σ describes the width of the PDF. If $\alpha = 2$, the FMLS process coincides with the BS model, where the BS volatility σ_{BS} is related to the dispersion measure for the FMLS model volatility σ_{FMLS} such that an equality is constructed as $\sigma_{BS} = \sqrt{2}\sigma_{FMLS}$.

Appendix A.2. Stochastic Volatility Model

There is a significant amount of literature in the research field of stochastic volatility (SV) models (e.g., Hull and White, 1987; Heston, 1993; Lewis, 2000; Lord and Kahl, 2010; Ackerer et al., 2016; Fonseca and Martini, 2016). In this paper, we use the one-dimensional affine Heston model (Heston, 1993), an affine stochastic volatility model, and its characteristic function (Lord and Kahl, 2010) as an example to demonstrate the feasibility of using the CFS method on pricing options under the SV models. The Heston SDE is defined as follows:

$$dL_t = \gamma_c dt + \sqrt{y_t}dW_{1,t}, \tag{A.23}$$

$$dy_t = \lambda(\bar{y} - y_t)dt + \eta\sqrt{y_t}dW_{2,t}, \tag{A.24}$$

where L_t and y_t denote the stochastic log-asset price variable and the variance of the asset price process, respectively. In this process, the speed of mean reversion λ, the mean level of variance $\bar{y}$ and the volatility of volatility η are constant values greater than or equal to zero. Additionally, the Brownian motions $W_{1,t}$ and $W_{2,t}$ are correlated with the correlation coefficient ρ_s. It is worth

mentioning the model characteristic function due to its relative complexity:

$$\begin{aligned}\mathbb{E}\left[e^{izL_t^{(\text{Heston})}}\right] &:= \phi(z) \\ &= \exp\left(iz\gamma_c t + \frac{y_0}{\eta^2}\left(\frac{1-e^{Et}}{1-Fe^{Et}}(\lambda - i\rho_s\eta z - E)\right) + \right. \\ &\left.\frac{\lambda\bar{y}}{\eta^2}\left(t(\lambda - i\rho_s\eta z - E) - 2\log(\frac{1-Fe^{-Et}}{1-F})\right)\right),\ z \in \mathbb{R} \end{aligned} \tag{A.25}$$

with

$$\begin{aligned}E =& \sqrt{(\lambda - i\rho_s\eta z) + (z^2 + iz)\eta^2}, \\ F =& (\lambda - i\rho_s\eta z - E)/(\lambda - i\rho_s\eta z + E).\end{aligned}$$

This characteristic function is uniquely specified because we take $\sqrt{(x+yi)}$ such that its real part is nonnegative and restrict the complex logarithm to its principal branch. In this case, as Lord and Kahl (2010) prove, the resulting characteristic function is the correct one for all complex numbers z in the analytic strip of the characteristic function. In the SDE, we have two possible conditions with respect to λ, $\bar{y}$ and η:

$$2\lambda\bar{y} \geq \eta^2, \tag{A.26}$$

$$2\lambda\bar{y} < \eta^2. \tag{A.27}$$

The model satisfies the Feller property if (A.26) holds; otherwise, (A.27) holds. If a process fulfils the property, the process never hits zero, but if it does not, this means that the process can reach 0. Condition (A.27) is a very important property for the Heston SDEs because the SDEs can only have a unique solution when we specify a boundary condition at 0. In mathematical finance, the chosen boundary condition is that the process remains at 0. We define this as the absorbing boundary condition. When the process reaches 0 and is allowed to leave 0, we call it a reflecting boundary. These two boundary conditions are crucial for pricing early-exercise options, including American options and barrier options.

Appendix B. Table of Cumulants

In Table B.18, we show the first c_1, second c_2, and fourth c_4 cumulants of the GB model, the Merton model, the Kou model, the Meixner Model, the NIG model, the VG model, the CGMY_e model and the FMLS model. However, as Fang and Oosterlee (2008) suggest, due to the lengthy representation of c_4, we only present the first two cumulants of the Heston model. In the CGMY_e model, we only present the cumulants when $Y \in (0,2)/\{1\}$ because when $Y = 0$, the CGMY_e model becomes the Kou model, and when $Y = 1$, it becomes the VG model. To obtain a pure

CGMY process, we can set σ equal to zero. Given the characteristic functions, the cumulants can be generally computed using

$$c_k = \frac{1}{i^k} \frac{\partial^k \log \phi(z)}{\partial z^n}\bigg|_{z=0}.$$

References

Ackerer, D., Filipović, D., Pulido, S., 2016. The Jacobi stochastic volatility model. Swiss Finance Institute Research Paper Series No. 16–35.

Almendral, A., 2004. Numerical valuation of American options under the CGMY process, in: Schoutens, W., Kyprianou, A., Wilmott, P. (Eds.), Exotic Option Pricing and Advanced Lévy Models. Wiley, UK, pp. 259–276.

Almendral, A., Oosterlee, C.W., 2005. Numerical valuation of options with jumps in the underlying. Applied Numerical Mathematics 53, 1–18.

Almendral, A., Oosterlee, C.W., 2006. Highly accurate evaluation of European and American options under the Variance Gamma process. Journal of Computational Finance 10, 21–42.

Almendral, A., Oosterlee, C.W., 2007. Accurate evaluation of European and American options under the CGMY process. SIAM Journal on Scientific Computing 29, 93–117.

Andersen, L., Andreasen, J., 2000. Jump-diffusion processes: Volalitility smile fitting and numerical methods for option pricing. Review of Derivatives Research 4, 231–262.

Bates, D.S., 1991. The crash of '87: Was it expected? The evidence from options markets. The Journal of Finance 46, 1009–1044.

Bates, D.S., 1996. Jumps and stochastic volatility: Exchange rate processes implicit in Deutsche Mark options. The Review of Financial Studies 9, 69–107.

Black, F., Scholes, M., 1973. The pricing of options and corporate liabilities. Journal of Political Economy 81, 637–654.

Boyd, J.P., 2003. Chebyshev and Fourier Spectral Methods. Dover Publications Inc., New York, USA.

Brummelhuis, R., Chan, R.T., 2014. A radial basis function scheme for option pricing in exponential Lévy models. Applied Mathematics Finance 21, 238–269.

Carmona, R., Durrleman, V., 2003. Pricing and hedging spread options. SIAM Review 45, 627–685.

Table B.18: The first c_1, second c_2, and fourth c_4 cumulants of various models.

Lévy models	
BS	$c_1 = (r - q + \omega)t \quad c_2 = \sigma^2 t, \quad c_4 = 0$, $\omega = -0.5\sigma^2$
Merton	$c_1 = (r - q + \omega - \lambda\mu_j)t$ $c_2 = (\sigma^2 + \lambda(\sigma_J^2 + \mu_J^2))t$ $c_4 = t\lambda(6\sigma_J^2\mu_J^2 + \mu_J^4 + 3\sigma_J^4\lambda)$ $\omega = -0.5\sigma^2 - \lambda\big(e^{\sigma_J^2/2+\mu_J} - 1\big)$
Kou	$c_1 = (r - q + \omega + p\lambda/\alpha_1 + \lambda(1-p)/\alpha_2)t$ $c_2 = (2\frac{\lambda p}{\alpha_1^2} + 2\frac{\lambda(1-p)}{\alpha_2^2})t$ $c_4 = 24\lambda(\frac{p}{\alpha_1^5} + \frac{1-p}{\alpha_2^5})t$ $\omega = -0.5\sigma^2 + \lambda\big(\frac{p\alpha_1}{\alpha_1+1} + \frac{(1-p)\alpha_2}{\alpha_2-1} - 1\big)$
Meixner	$c_1 = (r - q + \omega)t + \alpha dt\tan(\beta/2)$ $c_2 = \frac{\alpha^2 dt}{2}(\cos^{-2}\beta/2) - (\alpha dt\tan(\beta/2))^2$ $c_4 = \frac{3-2\cos^2(\beta/2)}{d} - 4\sin(\beta/2)\sqrt{2/dt}(\alpha dt\tan(\beta/2)) - 3(\frac{\alpha^2 dt}{2}(\cos^{-2}\beta/2))^2 +$ $\quad 12(\frac{\alpha^2 dt}{2}(\cos^{-2}\beta/2))(\alpha dt\tan(\beta/2))^2 - 6(\alpha dt\tan(\beta/2))^4$ $\omega = \Big(\frac{\cos(\beta/2)}{\cos((\alpha+\beta)/2)}\Big)^{2dt}$
NIG	$c_1 = (r - q + \omega)t + \delta t\beta/\sqrt{\alpha^2 - \beta^2}$ $c_2 = \delta t\alpha^2(\alpha^2 - \beta^2)^{-3/2}$ $c_4 = \delta t\alpha^2(\alpha^2 + 4\beta^2)^{-3/2}(\alpha^2 - \beta^2)^{-7/2}$ $\omega = -0.5\sigma^2 - \delta(\sqrt{\alpha^2 - \beta^2} - \sqrt{\alpha^2 - (\beta+1)^2})$
VG	$c_1 = (r - q + \theta + \omega)t$ $c_2 = (\sigma^2 + \upsilon\theta^2)t$ $c_4 = 3(\sigma^4\upsilon + 2\theta^4\upsilon^3 + 4\sigma^2\theta^2\upsilon^2)t$ $\omega = \frac{1}{\upsilon}\log(1 - \theta\upsilon - \sigma^2\upsilon/2)$
CGMY_e	$c_1 = (r - q + \omega)t$ $c_2 = (\sigma^2 + C\Gamma(2-Y)(M^{Y-2} + G^{Y-2})t$ $c_4 = (C\Gamma(4-Y)(M^{Y-4} + G^{Y-4})t$ $\omega = -0.5\sigma^2 + \Big(C\Gamma(-Y)G^Y\Big(\big(1 + \frac{1}{G}\big)^Y - 1 - \frac{Y}{G}\Big) + C\Gamma(-Y)M^Y\Big(\big(1 - \frac{1}{M}\big)^Y - 1 + \frac{Y}{M}\Big)\Big)$
FMLS	$c_1 = (r - q + \omega)t$ $c_2 = 0$ $c_4 = 0$ $\omega = (-1)^{\alpha+1}\sigma^\alpha\sec(\pi\alpha/2)$
Affine stochastic volatility model	
Heston	$c_1 = (r - q)t + (1 - e^{-\lambda t})\frac{\bar{y} - y_0}{2\lambda} - 0.5\bar{y}t$ $c_2 = \frac{1}{8\lambda^3}\Big(\eta t\lambda\exp(-\lambda t)(y_0 - \bar{y})(8\lambda\rho - 4\eta) +$ $\quad \lambda\rho\eta(1 - e^{-\lambda t})(16\bar{y} - 8y_0) + 2\bar{y}\lambda t(-4\rho\eta + \eta^2 + 4\lambda^2) +$ $\quad \eta^2((\bar{u} - 2u_0)e^{-2\lambda t} + \bar{y}(6e^{-\lambda t} - 7) + 2y_0) + 8\lambda^2(y_0 - \bar{y})(1 - e^{-\lambda t})\Big)$

Carr, P., Geman, H., Madan, D.B., Yor, M., 2002. The fine structure of asset returns: An empirical investigation. Journal of Business 75, 305–332.

Carr, P., Madan, D., 1991. Option valuation using the fast Fourier transform. Journal of Computational Finance 4, 61–73.

Carr, P., Wu, L., 2003. The finite moment log stable process and option pricing. Journal of Finance 58, 753–777.

Chan, R.T., 2016. Adaptive radial basis function methods for pricing options under jump-diffusion models. Computational Economics 47, 623–643.

Chan, R.T., Hubbert, S., 2014. Options pricing under the one-dimensional jump-diffusion model using the radial basis function interpolation scheme. Review of Derivatives Research 17, 161–189.

Cont, R., Tankov, P., 2004. Financial Modelling with Jump Processes. Chapman & Hall/CRC Financial Mathematics Series, Chapman & Hall/CRC, Boca Raton, FL.

Cont, R., Voltchkova, E., 2005. A finite difference scheme for option pricing in jump diffusion and exponential Lévy models. SIAM Journal on Numerical Analysis 43, 1596–1626.

d'Halluin, Y., Forsyth, P.A., Labahn, G., 2004. A penalty method for American options with jump diffusion processes. Numerische Mathematik 97, 321–352.

d'Halluin, Y., Forsyth, P.A., Vetzalz, K.R., 2005. Robust numerical methods for contingent claims under jump diffusion process. IMA Journal of Numerical Analysis 25, 87–112.

Duffie, D., Pan, J., Singleton, K., 2000. Transform analysis and asset pricing for affine jump-diffusions. Econometrica 68, 1343–1376.

Fang, F., Oosterlee, C.W., 2008. A novel pricing method for European options based on Fourier-cosine series expansions. SIAM Journal on Scientific Computing 31, 826–848.

Fang, F., Oosterlee, C.W., 2009. Pricing early-exercise and discrete barrier options by Fourier-cosine series expansions. Numerische Mathematik 114, 27–62.

Fang, F., Oosterlee, C.W., 2011. A Fourier-based valuation method for Bermudan and barrier options under Heston's model. SIAM Journal on Financial Mathematics 2, 439–463.

Fonseca, J.D., Martini, C., 2016. The α-hypergeometric stochastic volatility model. Stochastic Processes and their Applications 126, 1472–1502.

Grigelionis, B., 1999. Processes of Meixner type. Lithuanian Mathematical Journal 39, 33–41.

Heston, S.L., 1993. A closed-form solution for options with stochastic volatility with application to bond and currency options. Review of Financial Studies 6, 327–343.

Hirsa, A., Madan, D.B., 2004. Pricing American options under variance gamma. Journal of Computational Finance 7, 63–80.

Hull, J., White, A., 1987. The pricing of options on assets with stochastic volatilities. The Journal of Finance 42, 281–300.

Ikonen, S., Toivanen, J., 2007a. Componentwise splitting methods for pricing American options under stochastic volatility. International Journal of Theoretical and Applied Finance 10, 331–361.

Ikonen, S., Toivanen, J., 2007b. Efficient numerical methods for pricing American options under stochastic volatility. Numerical Methods for Partial Differential Equations 24, 104–126.

Kou, S.G., 2002. A jump diffusion model for option pricing. Management Science 48, 1086–1101.

Kudryavtsev, O., Levendorskiĭ, S., 2009. Fast and accurate pricing of barrier options under Lévy processes. Finance and Stochastics 13, 531–562.

Leentvaar, C., Oosterlee, C., 2008. Multi-asset option pricing using a parallel Fourier-based technique. Journal of Computational Finance 12, 1–26.

Levendorskiĭ, S., 2004. Early exercise boundary and option pricing in Lévy driven models. Quantitative Finance 4, 525–547.

Lewis, A., 2001. A simple option formula for general jump-diffusion and other exponential Lévy processes. `http://optioncity.net/pubs/ExpLevy.pdf`.

Lewis, A.L., 2000. Option Valuation under Stochastic Volatility. Finance Press, Newport Beach, CA.

Lipton, A., 2002. The vol smile problem. Risk 15, 61–66.

Longstaff, F.A., Schwartz, E.S., 2001. Valuing American options by simulation: A simple least-square approach. Review of Financial Studies 14, 113–147.

Lord, R., Fang, F., Bervoets, F., Oosterlee, C.W., 2008. A fast and accurate FFT-based method for pricing early-exercise options under Lévy processes. SIAM Journal on Scientific Computing 31, 1678–1705.

Lord, R., Kahl, C., 2010. Complex logarithms in Heston-like models. Mathematical Finance 20, 671–694.

Lukacs, E., 1987. Developments in Characteristic Function Theory. Oxford University Press, Oxford, UK.

Luke, Y.L., 1969. The Special Functions and Their Approximations: VV.1. volume 53A of *Mathematics in Science and Engineering*. Academic Press, New York.

Madan, D.B., Carr, P., Chang, E.C., 1998. The variance gamma process and option pricing. European Finance Review 2, 79–105.

Madan, D.B., Milne, F., 1991. Option pricing with V. G. martingale components. Mathematical Finance 1, 39–55.

Madan, D.B., Seneta, E., 1990. The variance gamma (V.G.) model for share market returns. Journal of Business 63, 511–524.

Merton, R.C., 1973. Theory of rational option pricing. The Bell Journal of Economics and Management Science 4, 141–183.

Merton, R.C., 1976. Option pricing when underlying stock returns are discontinuous. Journal of Financial Economics 3, 125–144.

O'Sullivan, C., O'Sullivan, S., 2013. Pricing European and American options in the Heston model with accelerated explicit finite differencing methods. International Journal of Theoretical and Applied Finance 16, 135–170.

Rubinstein, M., 1985. Nonparametric tests of alternative option pricing models using all reported trades and quotes on the 30 most active cboe option classes from August 23, 1976 through August 31, 1978. The Journal of Finance 40, 455–480.

Rubinstein, M., 1994. Implied binomial trees. The Journal of Finance 49, 771–818.

Ruijter, M., Versteegh, M., Oosterlee, C., 2013. On the application of spectral filters in a Fourier option pricing technique. `http://ta.twi.tudelft.nl/mf/users/oosterle/oosterlee/main_v6.pdf`.

Ruijter, M.J., Oosterlee, C.W., 2015. A Fourier cosine method for an efficient computation of solutions to BSDEs. Journal of Computational Finance 37, A859–A889.

Schoutens, W., 2002. The Meixner Process: Theory and applications in finance. Technical Report 2002–004. Department of Mathematics, Katholieke Universiteit Leuven. Leuven, Belgium.

Schoutens, W., 2003. Lévy Processes in Finance: Pricing Financial Derivatives. Wiley Series in Probability and Mathematical Statistics, Wiley, Chichester, UK.

Schoutens, W., Teugels, J.L., 1998. Lévy processes, polynomials and martingales. Communications in Statistics - Stochastic Models 14, 335–349.

Tadmor, E., Tanner, J., 2005. Adaptive filters for piecewise smooth spectral data. IMA Journal of Numerical Analysis 25, 635–647.

Tankov, P., Voltchkova, E., 2009. Jump-diffusion models: A practitioner's guide. `http://people.math.jussieu.fr/~tankov/tankov_voltchkova.pdf`.

Vandeven, H., 1991. Family of spectral filters for discontinuous problems. Journal of Scientific Computing 6, 159–192.

Wang, I.R., Wan, J.W.L., Forsyth, P.A., 2007. Robust numerical valuation of European and American options under the CGMY process. Journal of Computational Finance 10, 31–69.

Zhang, B., Oosterlee, C.W., 2013. Efficient pricing of European-style Asian options under exponential Lévy processes based on Fourier cosine expansions. SIAM Journal on Financial Mathematics 4, 399–426.